P516691.PDF [Page: 3 of 54]

Copy No. 10

DEFENCE R&D DÉFENSE

INVESTIGATION OF RANGE DEPENDENT UNDERWATER ACOUSTIC RAY MODELS

A. Purcell
Anthony Purcell Consultants
P.O. Box 1388
Lunenburg, Nova Scotia B0J 2C0

Contract # W7707-00-8696

Defence R&D Canada
DEFENCE RESEARCH ESTABLISHMENT ATLANTIC

Contractor Report
DREA CR 2001-136

September 2001

National Defence / Défense nationale

Canada

P516691.PDF [Page: 4 of 54]

Copy No: _____

Investigation of Range Dependent Underwater Acoustic Ray Models

Anthony Purcell
Anthony Purcell Consultants
PO Box 1388
Lunenburg, Nova Scotia B0J 2C0

Contract # W7707-00-8696

The scientific or technical validity of this Contract Report is entirely the responsibility of the contractor and the contents do not necessarily have the approval or endorsement of Defence R & D Canada

Defence Research Establishment Atlantic

Contractor Report

DREA CR 2001-136

September 2001

P516691.PDF [Page: 5 of 54]

Author

Anthony Purcell

Approved by

David M. F. Chapman

Head Naval Sonar Section

Approved for release by

Kirk Foster

Chair Document Review Panel

© Her Majesty the Queen as represented by the Minister of National Defence, 2001

© Sa majesté la reine, représentée par le ministre de la Défense nationale, 2001

P516691.PDF [Page: 6 of 54]

Abstract

This report is an annotated bibliography of ray theory approaches to the analysis of high frequency, shallow water propagation. Specifically, it is concerned with the calculation of the ray paths, travel times, arrival angles and coherent transmission losses for range-dependent velocity profile, variable bathymetry, and shallow water environments. The two approaches considered are the classic ray theory and the Gaussian beam method. The software developed in this report to evaluate the feasibility of applying these models to range-dependent environments is based on the numerical solution of the differential ray equations rather than analytic solutions of the ray paths for special cases. The ocean surface is assumed to be a flat pressure-release surface; the ocean bottom is a rigid, arbitrary bathymetry surface. The number of allowed surface or bottom bounces is adjustable and arbitrary. All parameters have cylindrical symmetry so there is propagation only in the same plane. The specific cases considered are the Gordon and Pedersen profile, the Munk profile, and a range-dependent, variable bathymetry, shallow water environment referred to as Scenario 5.

Résumé

Le présent rapport est une bibliographie annotée des méthodes d'analyse de la propagation des hautes fréquences en eau peu profonde, basées sur la théorie des rayons. Plus particulièrement, il porte sur le calcul des trajets de rayons, les temps de propagation, les angles d'incidence et les pertes d'émission cohérente pour le profil de vitesse du son dépendant de la distance, la bathymétrie variable et les milieux d'eau peu profonde. Les deux méthodes considérées sont la théorie classique des rayons et la méthode du faisceau gaussien. Le logiciel développé pour évaluer la faisabilité d'appliquer ces modèles à des milieux dépendant de la distance est basé sur la résolution numérique des équations de rayons différentielles plutôt que sur les résolutions analytiques des trajets de rayons de cas particuliers. Il est présumé que la surface océanique est une surface plate de libération de pression; le fond océanique est une surface bathymétrique rigide arbitraire. Le nombre de réflexions sur la surface ou sur le fond est réglable et arbitraire. Tous les paramètres ont une symétrie cylindrique, de sorte qu'il y a propagation dans un même plan seulement. Les cas particuliers étudiés sont le profil de Gordon et Pedersen, le profil de Munk et un milieu d'eau peu profonde à bathymétrie variable dépendant de la distance et désigné scénario 5.

16691.PDF [Page: 7 of 54]

104-07019/

This page intentionally left blank.

P516691.PDF [Page: 8 of 54]

Executive summary

In the early days of naval sonar modelling, much was accomplished through the use of "ray" models based on geometrical acoustic approximations to solutions to the wave equation. Ray models are intuitive and are fairly rapid to implement in range-independent media. Interest in the lower frequencies of passive sonar and enhanced treatment of seabed effects drove model development in the direction of "wave" solutions, such as normal modes, Parabolic Equation, and other models. Recently, renewed interest in active sonar has led to a resurrection of ray-based models, although now users are demanding that the models handle range-dependent media. The emphasis on operation in shallow (i.e., continental shelf) waters implies range-dependence both through natural variation of the oceanic sound speed profile and the variation on water depth. These considerations pose significant challenges to the latter-day ray modeller.

The thrust of this research contract was to investigate the mathematical modelling of range-dependent ray theory, using an efficient high-level mathematical programming tool to validate the methods and results. Ray paths between source and receiver in a generic range-dependent environment were computed, including attributes such as travel time, signal level, and transmit and receive angles. Special attention was given to the treatment of variable bathymetry, including slope effects. Some effort was devoted to the Gaussian beam method, an enhanced ray technique used in some sonar models.

One outcome of the work was the re-discovery of a technique, which apparently has been used in seismology, but not in underwater acoustics: computing the transmission loss along a ray by integrating differential forms of the ray equations. Normally, transmission loss is computed by tracing adjacent rays having a finite difference of launch angle, and tracking the divergence of the rays along the path. This standard technique is prone to numerical error and the differential technique improves on this, at the cost of additional compute time (but this is not prohibitive).

The Gaussian beam method proved to be straightforward to implement, but the investigator turned up one or two details in the theory that have not been adequately resolved. In any case, the Gaussian beam method was shown to be a bettor descriptor of the acoustic field in the transition into a shadow zone, but not deep within the zone itself. However, this limitation would not be of much concern in a sonar model, and in any case it is a huge improvement over the classic ray method, which does not handle the transition into a shadow zone very well.

The investigations were performed using the software package Mathematica, which is appropriate for mathematical physics investigations of this type. The resulting Mathematica notebooks provide a useful scientific tool for R&D purposes: however additional work would

516691.PDF [Page: 9 of 54]

have to be done to implement the algorithms for the end user. (It was never the intent that the investigator would generate such software; rather, the intent was to validate the science and mathematics as a first step.)

Purcell, Anthony 2001
Investigation of Range-Dependent Underwater Acoustic Ray Models
DREA CR 2001
Anthony Purcell Consultants

PS16691.PDF [Page: 19 of 54]

Sommaire

Lors de l'avènement de la modélisation du sonar naval, on a fait de belles réalisations au moyen des modèles de rayons basés sur des approximations acoustiques géométriques aux solutions de l'équation d'onde. Les modèles de rayons sont intuitifs et permettent une mise en œuvre assez rapide dans des milieux indépendants de la distance. Comme on s'intéressait aux fréquences inférieures du sonar passif et au traitement perfectionné des effets du fond océanique, la modélisation s'est orientée vers des solutions « ondulaires », telles que les modes normaux, l'équation parabolique et autres modèles. Dernièrement, l'intérêt renouvelé pour le sonar actif a donné lieu à une résurrection de modèles basés sur les rayons, bien que les utilisateurs exigent maintenant que les modèles prennent en charge les milieux dépendant de la distance. L'accent mis sur le fonctionnement en eau peu profonde (c.-à-d. la plate-forme continentale) implique une dépendance de la distance tant en raison de la variation naturelle du profil de vitesse du son océanique qu'en raison de la variation de la profondeur. Ces considérations posent des défis considérables pour le modeleur moderne des rayons.

Le contrat de recherche en cause avait pour objet d'étudier la modélisation mathématique de la théorie des rayons dépendant de la distance au moyen d'un outil de programmation mathématique efficace de haut niveau pour valider les méthodes et les résultats. Les trajets des rayons entre la source et le récepteur dans un milieu générique dépendant de la distance ont été calculés, y compris des caractéristiques telles que le temps de propagation, l'intensité du signal et les angles d'émission et de réception. Une attention particulière a été accordée au traitement de la bathymétrie variable, y compris les effets de pente. Un certain effort a été consacré à la méthode du faisceau gaussien, une technique des rayons perfectionnée utilisée pour certains modèles sonar.

Un des dividendes du travail était la redécouverte d'une technique qui a apparemment été utilisée en sismologie, mais non en acoustique sous-marine : calcul des pertes de transmission le long d'un rayon au moyen de l'intégration de formes différentielles des équations des rayons. Normalement, on calcule les pertes de transmission en traçant les rayons voisins ayant une différence finie d'angle d'émission et en notant la divergence des rayons le long de leur trajet. Cette technique standard est susceptible d'erreurs numériques, et la technique différentielle constitue une amélioration, sauf qu'elle exige un temps de calcul supplémentaire (qui n'est pas exorbitant).

La méthode du faisceau gaussien s'est avérée facile à mettre en œuvre, mais le chercheur a détecté un ou deux détails de la théorie qui n'ont pas été résolus de façon satisfaisante. De toute manière, on a démontré que la méthode du faisceau gaussien était un meilleur indicateur du champ acoustique dans la zone de transition vers une zone d'ombre, mais non à l'intérieur même de cette zone-ci. Toutefois, cette limitation ne poserait pas un grand problème dans un modèle sonar et, de toute façon, il s'agit d'une énorme amélioration par rapport à la méthode des rayons classique, qui ne prend pas très bien en charge la transition vers une zone d'ombre.

Les recherches ont été effectuées au moyen du progiciel Mathematica, qui convient bien à ce genre de recherches en physique mathématique. Les blocs-notes de Mathematica qui en résultent

516691.PDF [Page: 11 of 54]

constituent un outil scientifique utile aux fins de la R-D; cependant, il faudrait du travail supplémentaire pour mettre en œuvre les algorithmes pour l'utilisateur final. (Notre intention n'a jamais été que le chercheur produise un tel logiciel; il s'agissait simplement de valider la science et les mathématiques à titre de première étape.)

Purcell, Anthony 2001
Investigation of Range-Dependent Underwater Acoustic Ray Models
CRDA CR 2001
Anthony Purcell Consultants

P516691.PDF [Page: 12 of 54]

Contents

1 CLASSIC RAY THEORY 7

1.1 The ray equations 7

1.2 The coherent transmission loss 9

2 THE PORTER AND BUCKER IMPLEMENTATION OF THE GAUSSIAN BEAM METHOD 13

2.1 The "p-q" equations 13

2.2 Other variants of the Gaussian beam method 17

3 NUMERICAL RESULTS 19

3.1 The Gordon and Pedersen Profile 19

3.2 The Munk Profile 22

3.3 Comments on the Gordon and Pedersen and Munk cases 23

3.4 The shallow water case: Scenarios 1-5 26

4 CONCLUSIONS 35

P516691.PDF [Page: 13 of 54]

List of Figures

1.1 Definition of the coordinates. 8

3.1 The sound speed profile for the Gordon and Pedersen profile. The depth is in yards and the sound speed is in yards per second. 19
3.2 The ray trace for the shallow source case for the Gordon and Pedersen profile. The depth and range are in yards 20
3.3 The coherent transmission loss for the shallow source case for the Gordon and Pedersen profile, calculated using the Gaussian beam method (Eq. (2.34)). The range is in yards. The parameter values are summarized in Table 3.1. Compare this figure with Fig. 3 (c) of Porter and Bucker[5]. 21
3.4 The coherent transmission loss for the shallow source case for the Gordon and Pedersen profile, calculated using the classic ray theory method (Eq. (1.14)). The range is in yards. The parameter values are summarized in Table 3.1. Compare this figure with Fig. 3 (a) of Porter and Bucker[5]. 21
3.5 The ray trace for the deep source case for the Gordon and Pedersen profile. The depth and range are in yards. 22
3.6 The coherent transmission loss for the deep source case for the Gordon and Pedersen profile, calculated using the Gaussian beam method (Eq. (2.34)). The range is in yards. The parameter values are summarized in Table 3.2. Compare this figure with Fig. 5 (c) of Porter and Bucker[5] 23
3.7 The sound speed profile for the Gordon and Pedersen profile. The depth is in meters and the sound speed is meters per second. 24
3.8 The ray trace for the Munk profile. The range and depth are in meters. 24
3.9 The coherent transmission loss for the Munk profile, calculated using the Gaussian beam method. The range is in meters and the input parameters are summarized in Table 3.3. Compare this figure with Fig. 8 (c) of Porter and Bucker[5] 25
3.10 The coherent transmission loss for the Munk profile, calculated using the classic ray theory method. The range is in meters and the input parameters are summarized in Table 3.3. Compare this figure with Fig. 8 (a) of Porter and Bucker[5]. 25
3.11 Shallow water scenarios for ray theoretic analysis. 27
3.12 A least squares fit of exponentials (see Eq. (3.3)) to the data in Table 3.4. The depth is in meters and the sound speed is in meters per second. 29

P516691.PDF [Page: 14 of 54]

3.13 The ray trace for Scenario 5, for a source located in the upper duct at depth $z = 5$ m. There are 51 rays evenly spaced between $-5^o \leq \theta \leq 5^o$. The rays are terminated after 1 surface or 1 bottom bounce. 30
3.14 The ray trace for Scenario 5, for a source located in the upper duct at depth $z = 5$ m. There are 51 rays evenly spaced between $-5^o \leq \theta \leq 5^o$. The rays are terminated after 100 surface or 4 bottom bounces. 31
3.15 The ray trace for Scenario 5, for a source located in the lower duct at depth $z = 140$ m. There are 51 rays evenly spaced between $-5^o \leq \theta \leq 5^o$. The rays are terminated after 1 surface or 1 bottom bounce 31
3.16 The ray trace for Scenario 5, for a source located in the lower duct at depth $z = 140$ m. There are 51 rays evenly spaced between $-5^o \leq \theta \leq 5^o$. The rays are terminated after 100 surface or 4 bottom bounces 32
3.17 The coherent transmission loss for the deep source case for Scenario 5, calculated using the Gaussian beam method. There are 501 rays evenly distributed over initial angles $-5^o \leq \theta \leq 5^o$. The rays are terminated after 1 surface or 1 bottom bounce. The input parameters are given in Table 3.5. 33
3.18 The coherent transmission loss for the deep source case for Scenario 5, calculated using the classic ray theory method. There are 501 rays evenly distributed over initial angles $-5^o \leq \theta \leq 5^o$. The rays are terminated after 1 surface or 1 bottom bounce. The input parameters are given in Table 3.5. 33

P516691.PDF [Page: 15 of 54]

List of Tables

3.1 The parameters for the shallow source case for the Gordon and Pedersen profile. . . . 20
3.2 The parameters for the deep source case for the Gordon and Pedersen profile. 22
3.3 The input parameters for the Munk profile case. 23
3.4 The sound speed data for Profiles A and B. 26
3.5 The input parameters for Scenario 5. 32

P516691.PDF [Page: 16 of 54]

INTRODUCTION

The purpose of this report is to examine the classic ray theory approach and the Gaussian beam method (developed by Cerveny[1, 2, 3, 4], Porter and Bucker[5] and others[6],[7],[8] and determine whether these methods can be adapted to a range-dependent velocity profile, variable ocean bottom relief, shallow water environment. The idea is to allow arbitrary numbers of ocean surface and ocean bottom bounces and keep track of all multipath rays

To evaluate both models, the contractor has developed software to numerically solve the classic ray equations and also the additional "$p - q$" equations of the Gaussian beam method. The software is set up to allow arbitrary velocity profiles, rather than to take advantage of those special velocity profile cases where the ray paths and the $(p - q)$ variables can be solved for analytically. As well, the software correctly keeps track of the reflections from the arbitrary bottom relief and the ocean surface. The user can select the allowed number of ocean surface and ocean bottom reflections before the ray terminates. Useful quantities such as the ray paths, the travel times (the phase delay that is) and arrival angles of the rays emerge in a natural fashion from the numerical solution of the ray equations.

In classic ray theory one can calculate the coherent (or incoherent) transmission losses by examining the spreading of nearby rays. By considering the infinitesimal form of the geometrical spreading loss formula, one in effect differentiates the ray equations with respect to the initial grazing angle of the ray. Hence in classical ray theory one effectively doubles the number of differential equations to be solved in order to determine the transmission loss. For the coherent transmission loss one needs the the travel time (phase delay) as well, so this adds an additional equation. One ends up solving for 7 first order differential equations. In addition, to determine the transmission loss at a particular field point, one must determine which rays cross that point. In effect, one must invert the ray equations to find the initial angles of those rays which cross the field point.

In the Gaussian beam method the solution of the classical ray paths give the trajectories of the centers of the beams. The width and curvature of a beam is determined by solving for the $(p - q)$ variables along each beam. These are complex variables so that adds an additional 4 first order differential equations. Along with the time delay that gives a total of 8 first order equations. The total pressure at a field point is determined by adding up all the contributions to the pressure from each of the beams. One must calculate the distance along the normal from the beam center (the classic ray path) to the field point. This is the analog of the inversion problem for classical ray theory, but a much more tractable one. In some cases, an individual beam can make two separate contributions to the pressure at the same field point.

In addition, for each reflection (both in classic ray theory and Gaussian beam theory) the appropriate boundary conditions for these variables must be imposed to determine the new starting values of these variables after reflection. The combination of all these factors gives a weighty machinery of programming requirements. Even given the exploratory nature of these current investigations, the software presented in

P516691.PDF [Page: 17 of 54]

this contract is moderately complicated. The scope for improvements, modifications, and speed increases in the software used to evaluate both classic ray theory and the Gaussian beam method is essentially unlimited.

The review of the equations of classic ray theory, including those needed for the calculation of coherent transmission loss, is presented in Chapter 1. A detailed discussion of Porter and Bucker's implementation of the Gaussian beam method is given in Chapter 2. A brief discussion of some of the variants of the Gaussian beam method is given at the end of Chapter 2. The numerical results for the shallow source and deep source cases for the Gordon and Pedersen profile, the Munk profile and the range-dependent Scenario 5 case are presented in Chapter 3. Chapter 4 concludes the report with some general comments on the classic ray theory and Gaussian beam methods and a discussion of some technical issues that need to be examined. Copies of the complete software for calculating the ray paths and transmission loss are given in disk form. A list of the main references used by the author for the classic ray theory and the Gaussian beam method is given in the Bibliography. Note that the Bibliography is not in any sense complete, a search of the literature over the last 15 years, reveals some 400 references with the phrase "Gaussian beam" in the abstracts. There is a vast literature on Gaussian beams in the seismological, acoustical and optical fields.

Chapter 1

CLASSIC RAY THEORY

1.1 The ray equations

The generic case of interest, consists of a water column bounded by the ocean surface at $z = 0$ and the ocean bottom, whose profile is described by the relief function $z = d(r)$, as shown in Fig. 1.1. The case to be considered in this report (the case considered by Porter and Bucker[5]), is the spherical source in a cylindrically symmetric medium, so there is propagation only in the same plane. The speed of sound can depend only on the range r and the depth z, $c = c(r, z)$.

The ray equations are essentially a rewriting of the Eikonal equation, whose derivation can be found in many sources: for example see the elementary treatment in Sec. 5.13 in *Fundamentals of Acoustics* by Kinsler[9]. In a nutshell, one starts from the wave equation $\nabla^2 P = (1/c^2)\partial^2 P/\partial t^2$, and assumes a solution in the form of a plane wave $P = A(x, z)e^{i\omega[t - \Gamma(x,z)/c_0]}$. Assuming that the amplitude $A(x, z)$ and the phase $\Gamma(x, z)$ are slowing varying functions of position leads one from the wave equation to the Eikonal equation $\vec{\nabla}\Gamma \cdot \vec{\nabla}\Gamma = (c_0/c)^2$, which can easily be rewritten in the form of the standard ray equations.

The ray equations can be written in a number of equivalent forms, depending on the set of dependent variables chosen. In this report the variables chosen will be the ray coordinates $r = r(s)$, $z = z(s)$, the local grazing angle of the ray $\phi = \phi(s)$ and the travel time $\tau = \tau(s)$, where the independent variable is the arclength s along the particular ray. It is also understood that these dependent variables depend on the initial grazing angle of the ray i.e. $r = r(\theta, s)$, $z = z(\theta, s)$, $\phi = \phi(\theta, s)$ and $\tau = \tau(\theta, s)$. The θ dependence is suppressed unless it is required. Strictly speaking τ is not the travel time but the phase delay. For example after a reflection from the pressure-release ocean surface it is customary to keep track of the reflection coefficient $R = -1$ by adding $-\pi/\omega$ to τ. With these dependent variables the ray equations take the form

$$\frac{dr}{ds} = \cos[\phi(s)], \tag{1.1}$$

$$\frac{dz}{ds} = \sin[\phi(s)], \tag{1.2}$$

$$\frac{d\phi}{ds} = \frac{\sin[\phi(s)]}{c(r,z)}\frac{\partial c(r,z)}{\partial r} - \frac{\cos[\phi(s)]}{c(r,z)}\frac{\partial c(r,z)}{\partial z}, \tag{1.3}$$

$$\frac{d\tau}{ds} = \frac{1}{c(r,z)}. \tag{1.4}$$

P516691.PDF [Page: 19 of 54]

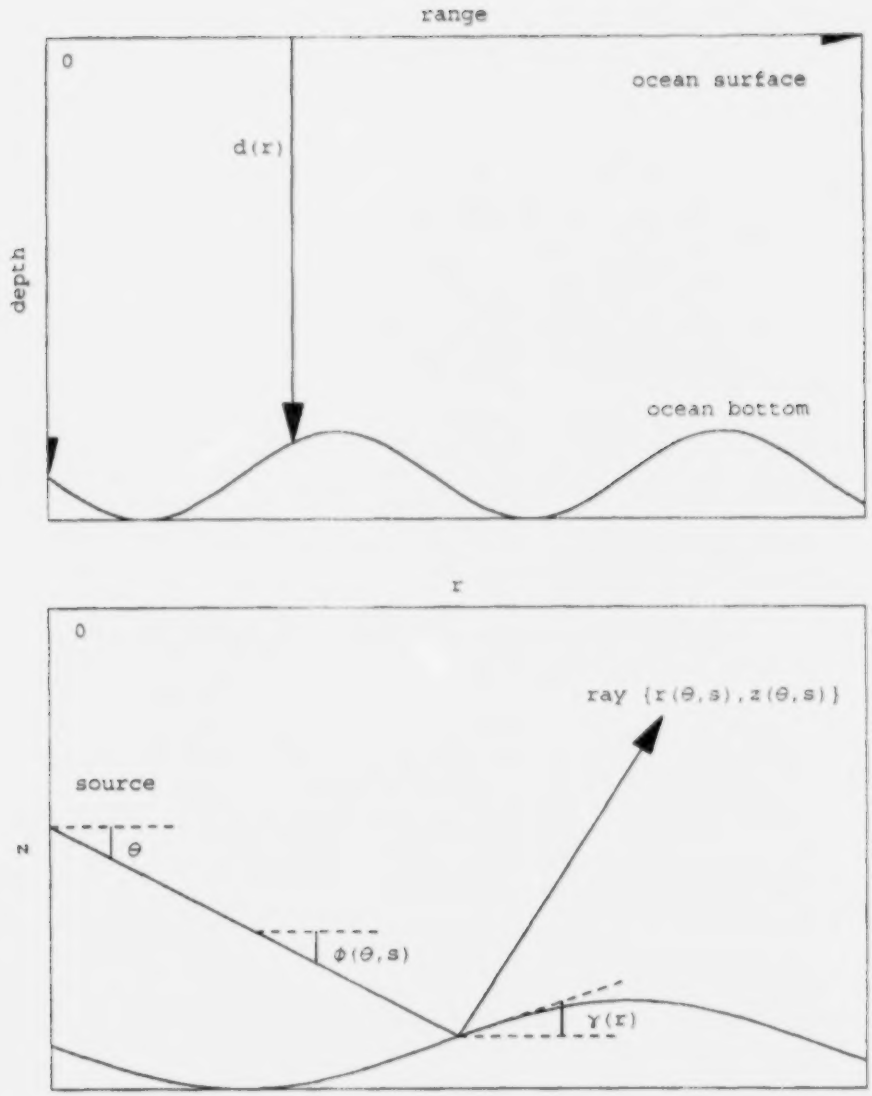

Figure 1.1: The geometry for ray theoretic approaches to shallow water propagation.

P516691.PDF [Page: 20 of 54]

The initial values of these first order equations are given by

$$r(0) = \text{source range}, \tag{1.5}$$

$$z(0) = \text{source depth}, \tag{1.6}$$

$$\tau(0) = 0, \tag{1.7}$$

$$\phi(0) = \theta, \tag{1.8}$$

where θ is the initial grazing angle, measured in the downward direction, as shown in Fig. 1.1

Now suppose that the ray reflects from a surface at some value of the arclength s_0 say; the boundary conditions are given by

$$r_{\rm new}(s_0) = r_{\rm old}(s_0), \tag{1.9}$$

$$z_{\rm new}(s_0) = z_{\rm old}(s_0). \tag{1.10}$$

$$\tau_{\rm new}(s_0) = \begin{cases} \tau_{\rm old}(s_0) - \pi/\omega, & \text{if } z_{\rm old}(s_0) = 0, \\ \tau_{\rm old}(s_0), & \text{if } z_{\rm old}(s_0) = d(r_{\rm old}(s_0)). \end{cases} \tag{1.11}$$

$$\phi_{\rm new}(s_0) = \begin{cases} -\phi_{\rm old}(s_0), & \text{if } z_{\rm old}(s_0) = 0, \\ -[\phi_{\rm old}(s_0) - 2\gamma(r_{\rm old}(s_0))], & \text{if } z_{\rm old}(s_0) = d(r_{\rm old}(s_0)). \end{cases} \tag{1.12}$$

If the ray reflects from the ocean surface subtract $\pi/(2\pi frequency)$ from the travel time. The angle $\gamma(r_{\rm old}(s_0))$ is (minus) the local tangent angle of the ocean bottom: if the ray reflects from the ocean bottom, subtract twice the local bottom tangent angle from the local ray grazing angle. The ocean bottom tangent angle is related to the bottom relief $z = d(r)$ by

$$\gamma(r) = -\arctan\left[\frac{\partial d(r)}{\partial r}\right]. \tag{1.13}$$

1.2 The coherent transmission loss

If all one is interested in are the ray paths and the travel times then these equations are complete. However to obtain the coherent transmission loss it is convenient (but not essential) to introduce additional equations. From Ugincius[10, 11, 12] one obtains the result that the intensity due to a single ray with initial angle θ and arclength s is given by

$$\frac{I(\theta, s)}{I_{\rm ref}} = \frac{1}{\left|\cos\phi(s)\frac{dz(\theta,s)}{d\theta} - \sin\phi(s)\frac{dr(\theta,s)}{d\theta}\right| \int_0^s ds'\, c[z(\theta,s'), r(\theta,s')]/c[z(0), r(0)]}. \tag{1.14}$$

This last result is just Eq. (20) of Ugincius[12]. One should also note that similar expressions have been developed in the literature by Eby[13], Anderson[14], Chen[15] and MacKinnon[16]. Note that an approximation for I/I_{ref} has also been given by Ugincius (Eq. (6) of [10]) and others in the form

$$\frac{I(\theta, s)}{I_{\rm ref}} = \frac{\cos\theta}{\left|\cos\phi(s)\frac{dz(\theta,s)}{d\theta} - \sin\phi(s)\frac{dr(\theta,s)}{d\theta}\right| (r(s) - r(0))} \tag{1.15}$$

This last expression is valid in the range-independent case, where Snell's law holds. Eq. (1.15) is easier to evaluate: however it is Eq. (1.14) that is used in this report.

516691.PDF [Page: 21 of 54]

In the case of multiple rays $\{(\theta_1, s_1), (\theta_2, s_2), \ldots\}$ crossing the same field point, the coherent intensity is then given by Eq. (24) of Gordon and Pedersen[17] as

$$\text{Transmission Loss} = \tag{1.16}$$
$$-10\log\left\{\frac{I(\theta_1,s_1)}{I_{\text{ref}}}+\frac{I(\theta_2,s_2)}{I_{\text{ref}}}+\cdots+2\cos[\omega(\tau(\theta_1,s_1)-\tau(\theta_2,s_2))]\sqrt{\frac{I(\theta_1,s_1)}{I_{\text{ref}}}}\sqrt{\frac{I(\theta_2,s_2)}{I_{\text{ref}}}}+\cdots\right\}.$$

The upshot of all this, is that one must introduce equations for the variables $dr(\theta,s)/d\theta$, $dz(\theta,s)/d\theta$ and $d\phi(\theta,s)/d\theta$ (although $d\phi(\theta,s)/d\theta$ does not enter directly into the transmission loss, it is coupled into the equations for $dr(\theta,s)/d\theta$, $dz(\theta,s)/d\theta$). One obtains the equations and the boundary conditions simply by differentiating Eqs. (1.1)-(1.3) with respect to θ. One obtains the additional relations:

$$\frac{d}{ds}\begin{bmatrix}\frac{dr}{d\theta}\end{bmatrix} = -\sin[\phi]\begin{bmatrix}\frac{d\phi}{d\theta}\end{bmatrix}, \tag{1.17}$$

$$\frac{d}{ds}\begin{bmatrix}\frac{dz}{d\theta}\end{bmatrix} = \cos[\phi]\begin{bmatrix}\frac{d\phi}{d\theta}\end{bmatrix}. \tag{1.18}$$

$$\begin{aligned}\frac{d}{ds}\begin{bmatrix}\frac{d\phi}{d\theta}\end{bmatrix} = &\left[\frac{\sin[\phi]}{c(r,z)}\left\{c_{rr}-\frac{c_r^2}{c(r,z)}\right\}-\frac{\cos[\phi]}{c(r,z)}\left\{c_{zr}-\frac{c_rc_z}{c(r,z)}\right\}\right]\begin{bmatrix}\frac{dr}{d\theta}\end{bmatrix}+\\ &\left[\frac{\sin[\phi]}{c(r,z)}\left\{c_{rz}-\frac{c_rc_z}{c(r,z)}\right\}-\frac{\cos[\phi]}{c(r,z)}\left\{c_{zz}-\frac{c_z^2}{c(r,z)}\right\}\right]\begin{bmatrix}\frac{dz}{d\theta}\end{bmatrix}\\ &\left[\frac{\cos[\phi]}{c(r,z)}c_r+\frac{\sin[\phi]}{c(r,z)}c_z\right]\begin{bmatrix}\frac{d\phi}{d\theta}\end{bmatrix}.\end{aligned} \tag{1.19}$$

where $c_r \equiv \partial c(r,z)/\partial r$ and so on.

The initial values of these first order equations are given by

$$\left.\frac{dr}{d\theta}\right|_{s=0} = 0, \tag{1.20}$$

$$\left.\frac{dz}{d\theta}\right|_{s=0} = 0, \tag{1.21}$$

$$\left.\frac{d\phi}{d\theta}\right|_{s=0} = 1. \tag{1.22}$$

Now suppose that the ray reflects from a surface at some value of the arclength s_0 say; the boundary conditions are given by

$$\left[\frac{dr(s_0)}{d\theta}\right]_{new} = \left[\frac{dr(s_0)}{d\theta}\right]_{old}, \tag{1.23}$$

$$\left[\frac{dz(s_0)}{d\theta}\right]_{new} = -\left[\frac{dz(s_0)}{d\theta}\right]_{old}, \tag{1.24}$$

$$\left[\frac{d\phi(s_0)}{d\theta}\right]_{new} = -\left\{\left[\frac{d\phi(s_0)}{d\theta}\right]_{old}+2\cot[\phi_{\text{old}}(s_0)]\frac{c_z[r(s_0),z(s_0)]}{c[r(s_0),z(s_0)]}\left[\frac{dz(s_0)}{d\theta}\right]_{old}\right\}. \tag{1.25}$$

These equations are given in Eqs. (34) of Ugincius[10], see also Sec.II of MacKinnon[16].

One must note that Eqs. (1.23)-(1.25) are for horizontal reflecting surfaces – flat surfaces. Ugincius did not give the boundary conditions for general rough interfaces. Anderson obtained partial results for flat

surfaces inclined at a constant slope, however these results are not directly applicable to the case in this report. In particular, Eqs. (34) of Ugincius must be generalized to an arbitrary rough surface in order to apply this method to allow arbitrary numbers of bottom bounces from a rough bottom. This generalization doesn't seem to have published in the open literature. On the other hand one can still use Eq. (1.14) and simply approximate the derivatives from the infinitesimal differences

$$\begin{aligned} \frac{dr(\theta,s)}{d\theta} &\approx r(\theta+\delta\theta,s)-r(\theta,s), \\ \frac{dz(\theta,s)}{d\theta} &\approx z(\theta+\delta\theta,s)-z(\theta,s), \\ \frac{d\phi(\theta,s)}{d\theta} &\approx \phi(\theta+\delta\theta,s)-\phi(\theta,s). \end{aligned} \tag{1.26}$$

The ray equations **are** formulated for arbitrary rough bottom relief, so the ray paths can be calculated for any number of bottom bounces. The inconvenience is in deciding what value of $\delta\theta$ is appropriate to use. The correct course of action is to attempt to generalize the boundary conditions Eqs. (1.23)-(1.25) to arbitrary rough surfaces. One can still use Eqs. (1.17)-(1.25) for arbitrary rough bottom relief if one terminates the rays after one bottom bounce, but still allows for arbitrary numbers of surface bounces.

In principal, this completes the all the input equations needed to calculate coherent transmission loss in a range dependent environment. However, there remains a difficult inversion problem to be solved. In Eq. (1.14), one must know what rays actually cross the particular field point. This is the exact opposite of what one normally carries out, namely given an initial θ and a particular value of the arclength, solve the differential ray equations for the field point $\{r(\theta,s),z(\theta,s)\}$. The strategy followed in the software accompanying this report, is as follows. First a fan of rays is calculated, each ray separated an some initial angle $\delta\theta$. Each pair of rays is searched until one finds those pairs (say $(\theta_1,\theta_1-\delta\theta)$) which bracket the field point. Then an interpolation scheme (cubic polynomials) is constructed from the four nearest neighbors to those bracketing rays $(\theta_1-\delta\theta,\theta_1,\theta_1+\delta\theta,\theta_1+2\delta\theta)$. This interpolation scheme holds s fixed and interpolates only with respect to θ. Then FindRoot[][18] is used, employing the bracketing rays as starting points in the root search (and also as a limit on the root search), until an exact value of θ and arclength s is found for an intersecting ray. For the rather weak refracting profiles and shallow depths considered in this report, it is sufficient to use $s\approx R_{receiver}$ as the starting point for the search for the arclength value of the ray which intersects the field point. Hence one is searching both the θ values and the arclength values using FindRoot[]. Once the values of (θ,s) are found, the values of $\tau(\theta,s)$ and $I(\theta,s)/I_{ref}$ along the intersecting ray are also found using a similar interpolation scheme. At this stage one could take just the values (θ,s) of the intersecting ray and re-solve the ray equations for the exact values of $\tau(\theta,s)$ and ray intensity, but this would be time consuming and doesn't offer an noticeable increase in accuracy.

The weakness of this scheme (and the place to make improvements) lies in the interpolation scheme. In other words, given a series of rays with initial angles θ_1, $\theta_1+\delta\theta$, $\theta_1+2\delta\theta$ etc., what is the best way to interpolate for intermediate values of θ? The scheme of keeping s fixed and interpolating only with respect to θ runs into difficulties at caustics or near shadow zones. A superior scheme would be to interpolate along the curves of constant grazing angle $\phi(\theta,s)$, allowing both θ and s to vary in the interpolation scheme. This method can be used right up to the edge of caustics and shadow zones with no difficulty. The drawback is that one must find efficient and robust numerical schemes to map out the curves of constant $\phi(\theta,s)$ through the $\theta-s$ plane. The contractor had some success in this endeavor, but had to abandon this idea due to time constraints. The construction of a more reliable interpolation scheme for intermediate values of θ is the

516691.PDF [Page: 23 of 54]

key to improving the inversion problem for ray acoustics. An improved inversion scheme would also allow a drastic reduction in the number of rays required, leading to a decrease in computational time.

For the the three cases considered in this report, the inversion scheme given in Appendix A (holding s fixed and using cubic polynomials to interpolate between different θ values) is quite accurate. Away from the edge of shadow zones, within cms for the Munk case and the range-dependent Scenario 5 case (over ranges of tens of kilometers), within a meter for the strongly refracting Gordon and Pedersen profile.

Chapter 2

THE PORTER AND BUCKER IMPLEMENTATION OF THE GAUSSIAN BEAM METHOD

2.1 The "p-q" equations

The derivation of the Gaussian beam equations can be found in Cerveny[1] and also in Porter and Bucker[5] Very briefly the derivation runs as follows. First, one starts from the wave equation for the pressure $P = P(r, z, t)$

$$\nabla^2 P = \frac{1}{c^2}\frac{\partial^2 P}{\partial t^2}. \tag{2.1}$$

Now change coordinates from the (r, z) coordinates to ray-centered coordinates (s, ν), where s is arclength along the particular ray, and $\nu = \omega^{1/2} n$ is the (scaled) normal distance from the ray center Hence one expresses $r = r(s, \nu)$ and $z = z(s, \nu)$ (the θ dependence is still there of course, so strictly speaking one should write $r = r(\theta, s, \nu)$ and $z = z(\theta, s, \nu)$). The idea is that these coordinates form a regular coordinate system in the immediate neighborhood of that particular ray One must transform the Laplacian in the wave equation to these new (s, ν) coordinates and also one makes the parabolic equation substitution

$$P(r, z, t) = \exp[-\iota\omega(\tau(s) - t)]U(s, \nu), \tag{2.2}$$

where $d\tau(s)/ds = 1/c$ so $\tau(s)$ is the travel time along that particular ray. Hence in the definition of τ one has $c = c(r(s, 0), z(s, 0)) \equiv c(s)$ since one is at the beam center $(\nu = 0)$ directly along the ray path. In the general case where one is not at the beam center one writes $c(r(s, \nu), z(s, \nu)) \equiv c(s, \nu)$ explicitly. This transforms the wave equation into the form

$$\omega^2 h\left(\frac{1}{c^2(s,\nu)} - \frac{1}{h^2 c^2}\right)U(s,\nu) + \omega\left[\frac{\iota c_s}{hc^2}U - \frac{\iota}{hc}U + hU_{\nu\nu} - \frac{\iota r_s}{rhc}U\right] +$$
$$\omega^{1/2}\left(U_\nu + \frac{r_\nu h}{r}U_\nu\right) + \frac{1}{h}U_{ss} - \frac{1}{h}U_s + \frac{r_s}{rh}U_s = 0, \tag{2.3}$$

where one has the notational device $h = 1 + (c_\nu(s, \nu)/c)\nu$. Now one expands the quantities $1/c^2(s, \nu)$ and $1/h(s, \nu)$ in a Taylor series around $\nu = 0$, substitutes these results into Eq. (2.3), and collects terms in powers of ω.

?516691.PDF [Page: 25 of 54]

One then seeks an asymptotic solution of the resulting equation in the form

$$U(s,\nu) = U^0(s,\nu) + U^1(s,\nu)/\omega^{1/2} + U^2(s,\nu)/\omega + \cdots \tag{2.4}$$

This is the key physical step in the Gaussian beam method, and this expansion can be related to the idea that the size of the first Fresnel zone (the region of the inhomogeneous medium separating the source and receiver that effects the propagation) is proportional to the wavelength. See for example the discussion in Cerveny[3] for a discussion of this point. To $O(\omega)$ one obtains

$$\left[-\left(\frac{c_{ss}}{c}\right)\nu^2 + \frac{ic_s}{c^2} - \frac{ir_s}{rc}\right] U^0 - \frac{2i}{c}U^0_s + U^0_{ss} = 0. \tag{2.5}$$

One then reduces this second order equation to two first order equations for the $(p-q)$ variables by introducing the transformation

$$U^0 = A_0\sqrt{c/(qr)}\exp[-i\nu^2 p/(2q)]. \tag{2.6}$$

The physical meaning of these $(p-q)$ variables is related to the beam half-width and the beam curvature respectively:

$$L(s) = \sqrt{-2/\{\omega\ \mathrm{Im}[p(s)/q(s)]\}}, \quad K(s) = -c[r(s),z(s)]\ \mathrm{Re}[p(s)/q(s)].$$

Finally, the full set of differential equations for the Gaussian beam method including the "p-q" equations is then given by:

$$\frac{dr}{ds} = \cos[\phi(s)], \tag{2.7}$$

$$\frac{dz}{ds} = \sin[\phi(s)], \tag{2.8}$$

$$\frac{d\phi}{ds} = \frac{\sin[\phi(s)]}{c(r,z)}\frac{\partial c(r,z)}{\partial r} - \frac{\cos[\phi(s)]}{c(r,z)}\frac{\partial c(r,z)}{\partial z}, \tag{2.9}$$

$$\frac{dt}{ds} = \frac{1}{c(r,z)}, \tag{2.10}$$

$$\frac{dq}{ds} = c(r,z)p(s), \tag{2.11}$$

$$\frac{dp}{ds} = -\frac{q(s)}{c(r,z)^2}[\sin^2\phi(s)\, c_{rr}(r,z) - 2\sin\phi(s)\cos\phi(s)\, c_{rz}(r,z) + \cos^2\phi(s)\, c_{zz}(r,z)]. \tag{2.12}$$

where

$$c_{rr}(r,z) = \partial^2 c(r,z)/(\partial r)^2,\ c_{rz}(r,z) = \partial^2 c(r,z)/\partial r\partial z,\ c_{zz}(r,z) = \partial^2 c(r,z)/(\partial z)^2.$$

The initial values of these first order equations are given by

$$r(0) = \text{source range}, \tag{2.13}$$

$$z(0) = \text{source depth}, \tag{2.14}$$

$$\tau(0) = 0, \tag{2.15}$$

$$\phi(0) = \theta, \tag{2.16}$$

$$p(0) = 1, \tag{2.17}$$

$$q(0) = i\,\frac{2\,c[r(0),z(0)]}{\omega(\delta\theta)^2}, \tag{2.18}$$

where θ is the initial grazing angle, measured in the downward direction. The parameter $\delta\theta$ is the separation of initial angles of the beam centers, which follow the classic ray paths.

Now suppose that the ray reflects from a surface at some value of the arclength s_0 say; the boundary conditions are given by

$$r_{\rm new}(s_0) = r_{\rm old}(s_0), \tag{2.19}$$

$$z_{\rm new}(s_0) = z_{\rm old}(s_0), \tag{2.20}$$

$$\tau_{\rm new}(s_0) = \begin{cases} \tau_{\rm old}(s_0) - \pi/\omega, & \text{if } z_{\rm old}(s_0) = 0, \\ \tau_{\rm old}(s_0), & \text{if } z_{\rm old}(s_0) = d(r_{\rm old}(s_0)). \end{cases} \tag{2.21}$$

$$\phi_{\rm new}(s_0) = \begin{cases} -\phi_{\rm old}(s_0), & \text{if } z_{\rm old}(s_0) = 0, \\ -[\phi_{\rm old}(s_0) - 2\gamma(r_{\rm old}(s_0))], & \text{if } z_{\rm old}(s_0) = d(r_{\rm old}(s_0)). \end{cases} \tag{2.22}$$

$$p_{\rm new}(s_0) = p_{\rm old}(s_0) + q(s)[ic_z(r,z)\cos^2\phi(s)/(c(r,z)\sin\phi(s))], \tag{2.23}$$

$$q_{\rm new}(s_0) = q_{\rm old}(s_0) \tag{2.24}$$

One must pay particular attention to Eq. (2.23); the form of the boundary condition for p at a reflecting surface was originally given by Cerveny as

$$p_{\rm new}(s_0) = p_{\rm old}(s_0) + q(s)N, \tag{2.25}$$

where

$$N = \left[2c_z(r,z)\cos\phi(s)\frac{\{2\sin^2\phi(s) - \cos^2\phi(s)\}}{c(r,z)\sin^2\phi(s)} - 2c_r(r,z)\frac{\cos^2\phi(s)}{c(r,z)\sin\phi(s)}\right] \tag{2.26}$$

This is Eq (60) of Cerveny[2] reduced to the case of a flat reflecting surface (in Cerveny's notation $N \equiv B$). The contractor has observed that this form gives incorrect results for the interference patterns for the Gordon and Pedersen profile. It is to Porter and Bucker's credit that they recognized this deficiency and empirically corrected Eq. (2.26) by multiplying this term by a factor of -2; this is probably the most valuable insight in Porter and Bucker's paper. Note that in the discussion following Eq. (22) of Porter and Bucker they state that they intend to publish a follow up paper on this matter. However, they did not do this (private communication June 2001). This does leave open the question of the correct form of this boundary condition for the full range-dependent case. One could try simplifying multiplying the entire N term by -2 and making a comparison with a known range-dependent benchmark case. For example there are a very useful series of range-dependent benchmark cases given recently in the Journal of the Acoustical Society by Thompson[19], Thompson and Brooke[20], Buckingham[21], Collins[22], Westwood[23], Jensen[24] and Stephen[25]. Alternatively one could re-examine the Cerveny derivation of Eq. (2.26) in detail and hope for some analytic insight. This was not possible in the time frame of this current contract. Cerveny does indeed give the boundary conditions for the general rough surface, however since his results are incorrect upon reduction to the flat interface, there is certainly no point in attempting to use his more general results, without a critical re-examination of his derivation of the boundary condition for p at a reflecting surface. The upshot of this is that one cannot reliably use the Cerveny method for multiple bounces from a rough surface.

The contribution to the pressure from each individual beam is given by

$$P(\theta) = \mathcal{E}\delta\left(\frac{1}{c(r,z)}\right)\exp(i\pi/4)\sqrt{\frac{q(0)\omega\cos\theta}{2\pi}}\sqrt{\frac{c(r,z)}{rq(s)}}\exp\{-i\omega[\tau + pn^2/(2q)]\} \tag{2.27}$$

P516691.PDF [Page: 27 of 54]

where $n(s)$ is the normal distance from the ray (the beam center) to the receiver point. The total pressure is just the sum of this expression over all beams.

$$P(receiver) = \sum_{\text{all rays}} P(\theta). \tag{2.28}$$

In effect, one must solve for those values of the arclength such that the normal projection from this point on the ray, intersects the field point. In fact, some individual rays can make two separate contributions to the same field point. The receiver coordinates appear in $P(\theta)$ only implicitly, through their determination of the values of the arclength. In effect the s that appears above is $s = s(R_{receiver}, Z_{receiver}, \theta)$, the r and z are the ray paths $r = r(\theta, s(R_{receiver}, Z_{receiver}, \theta))$, $z = z(\theta, s(R_{receiver}, Z_{receiver}, \theta))$ From simple geometry the values of the arclength which connect the normals to the receiver point are given by solving the equation

$$R_{receiver} = r(\theta, s) - [Z_{receiver} - z(\theta, s)] \tan[\varphi(\theta, s)] \tag{2.29}$$

(In fact Porter and Bucker find these s values by interpolation. The contractor constructed two versions of the software, one that follows Porter and Bucker and finds the arclength values by interpolation of "neighboring" families of normals, the other by explicitly solving the previous equation by using FindRoot[] in Mathematica. Both methods gave similar results. The software used to produce the graphs in this report use the interpolation method of Porter and Bucker. Probably the best solution would be some combination of these two methods.) Finally the values of the normal distance from the receiver to the rays are given by

$$n(\theta, s) = \sqrt{(R_{receiver} - r(\theta, s))^2 + (Z_{receiver} - z(\theta, s))^2}. \tag{2.30}$$

One must observe that the function $q(s)$ is complex and therefore the function $\sqrt{q(s)}$ is multiple-valued in the complex q-plane. To keep the phase of $P(\theta)$ continuous as a function of arclength, one chooses the branch of the square root such that

$$\sqrt{\frac{c(r,z)}{rq(s)}} = (-1)^{m(\theta,s)} \text{Principal Value}\left(\sqrt{\frac{c(r,z)}{rq(s)}}\right). \tag{2.31}$$

where Principal Value$(\sqrt{\frac{c(r,z)}{rq(s)}})$ denotes the usual principal value of the square root function that gives a phase in the range $\{-\pi, \pi\}$ and has a branch cut along the negative real axis. The function $m(\theta, s)$ is the integer number of times that $q(s)$ crosses the negative real axis. (In the Porter and Bucker manuscript, $m(\theta, s)$ is defined to be to be the number of times that $q(s)$ crosses the negative imaginary axis. This implies a different choice of the principal value function.) One should also note that keeping track of the appropriate branch of the square root involves tracking the entire history of the q variable, not simply its instantaneous value $q(s)$. The programming involved in defining $m(\theta, s)$, seems a little more difficult than indicated by Porter and Bucker.

In the cases investigated in this report, one allows for a fan of beams, whose beam centers are the classic ray solutions for rays whose initial angles are given by

$$\theta_k = \theta_{initial} + k\delta\theta; \text{ where } k = 0, 1, \ldots, n; \ \delta\theta = (\theta_{final} - \theta_{initial})/n \tag{2.32}$$

Hence there are $n + 1$ beams spanning the initial and final angles θ_{initial} and θ_{final}, each initial grazing angle separated by $\delta\theta$.

P516691.PDF [Page: 28 of 54]

Combining all these results one obtains for the total pressure

$$P(receiver) = \sum_{k=0}^{n} \sum_{\text{all } s} (-1)^{m(\theta\ s)} \exp(\imath\pi/4) \sqrt{\frac{\cos\theta}{\pi}} \sqrt{\frac{c(r,z)}{rq(s)}} \exp\{-\imath\omega[\tau + pn(s)^2/(2q)]\}. \tag{2.33}$$

where the sum $\sum_{\text{all } s}$ means all those solutions s which satisfy Eq (2.29). Finding these values s is the simpler analog of the classic ray inversion problem for the initial angles.

The coherent transmission loss is then just

$$TL = -10\log\left\{\left|\sum_{k=0}^{n} \sum_{\text{all } s} (-1)^{m(\theta\ s)} \exp(\imath\pi/4) \sqrt{\frac{\cos\theta}{\pi}} \sqrt{\frac{c(r,z)}{rq(s)}} \exp\{-\imath\omega[\tau + pn(s)^2/(2q)]\}\right|^2\right\} \tag{2.34}$$

To obtain the incoherent transmission loss, one takes the absolute value sign inside the double sum above i.e.

$$TL = -10\log\left\{\sum_{k=0}^{n} \sum_{\text{all } s} \left|\sqrt{\frac{\cos\theta}{\pi}} \sqrt{\frac{c(r,z)}{rq(s)}} \exp\{-\imath\omega[\tau + pn(s)^2/(2q)]\}\right|^2\right\}. \tag{2.35}$$

This completes the all the theory needed for Porter and Bucker's implementation of the Gaussian beam technique. The contractor has repeated the calculations of Porter and Bucker for the Gordon and Pedersen and Munk cases and succeeded in reproducing their results.

2.2 Other variants of the Gaussian beam method

There are four variants of the Gaussian beam method extant in the literature, these slightly different versions have been summarized in a recent review paper by Baxely, Bucker and Porter[26]. The differences between these approaches is best summarized by giving the form of the contribution to the pressure from an individual beam.

(a) The Cerveny method, developed by Porter and Bucker for acoustics, has been discussed in the previous section. The contribution of each beam to the pressure has the form

$$P(\theta) = \delta\theta \left(\frac{1}{c(r,z)}\right) \exp(\imath\pi/4) \sqrt{\frac{q(0)\omega\cos\theta}{2\pi}} \sqrt{\frac{c(r,z)}{rq(s)}} \exp\{-\imath\omega[\tau + pn^2/(2q)]\} \tag{2.36}$$

This is the most rigorous approach and it gives finite results even deep in the classic ray shadow zones.

(b) Simple Gaussian Beams developed by Bucker[6], gives the beam contribution to the pressure as

$$P(\theta) = \frac{\delta\theta}{s} \sqrt{\frac{a\cos\theta}{\pi}} \exp\{-\imath\omega\tau - a(n/s)^2\}, \tag{2.37}$$

where $a = -4\ln\{\mathcal{B}\}/(\delta\theta)^2$ and the "beam factor" $\mathcal{B}$ is chosen by the user

(c) Geometric Beam Tracing developed by Porter[7] gives the pressure due to a single beam as

$$P(\theta) = \begin{cases} \frac{W(s)-n}{W(s)} \sqrt{\frac{c}{c(\text{source})} \frac{\delta\theta}{r} \frac{\cos\theta}{|t|}} \exp\{-\imath\omega\tau\}, & n \le W(s), \\ 0, & \text{otherwise.} \end{cases} \tag{2.38}$$

where $W(s) = |q(s)\delta\theta/c(\text{source})|$. This model drops the beam strength to zero at the center of a neighboring ray.

P516691.PDF [Page: 29 of 54]

(d) Gaussian Ray Bundles introduced by Weinberg and Keenan[8], gives the beam contribution to the pressure as

$$P(\theta) = \frac{1}{(2\pi)^{1/4}} \sqrt{\frac{c}{c(\text{source})} \frac{\delta\theta}{r} \frac{\cos\theta}{W}} \exp[-(n/W)^2] \exp\{-\iota\omega\tau\}, \tag{2.39}$$

where $W = q(s)\delta\theta/c(\text{source})$.

In summary, the Simple Gaussian Beams, Geometric Beam Tracing and Geometric Ray Bundles methods are all slightly different simplifications of the Cerveny-Porter-Bucker approach. They are computationally more tractable but not as accurate in the classic ray shadow zones. Unless computational speed is essential the Cerveny-Porter-Bucker method is definitely superior.

P516691.PDF [Page: 30 of 54]

Chapter 3

NUMERICAL RESULTS

3.1 The Gordon and Pedersen Profile

The downward refracting profile of Gordon and Pedersen[17] is given by

$$c(z) = c_0\sqrt{1 - 2\gamma z/c_0}, \tag{3.1}$$

where $c_0 = 1677.3319$ yards/sec, $\gamma = -1.2286762$/sec. A plot of the profile is shown in Fig. 3.1

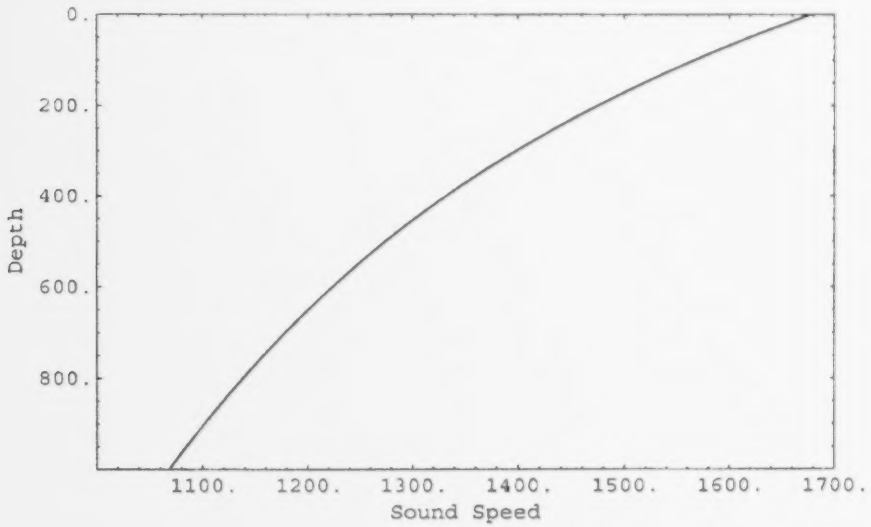

Figure 3.1: The sound speed profile for the Gordon and Pedersen profile. The depth is in yards and the sound speed is in yards per second.

The shallow source case input parameters are given in Table 3.1.

The ray trace for the shallow source case is shown in Fig. 3.2. The coherent transmission loss calculated using the Porter and Bucker method (Eq. (2.34)) is shown in Fig. 3.3. The classic ray theory result (Eq. (1.14)) for this case is shown in Fig. (3.4).

P516691.PDF [Page: 31 of 54]

The shallow source case:
source depth = 66.7 yards
source range =0 yards
receiver depth = 66.7 yards
receiver range ($500\ 0 \leq r \leq 1000\ 0$) yards
number of beams = 101. $(\theta_i, \theta_f) = (-25.0^o, 0^o)$
frequency = 2000.0 Hz
400 transmission loss points
MaxStepSize→10 yards

Table 3.1: The parameters for the shallow source case for the Gordon and Pedersen profile.

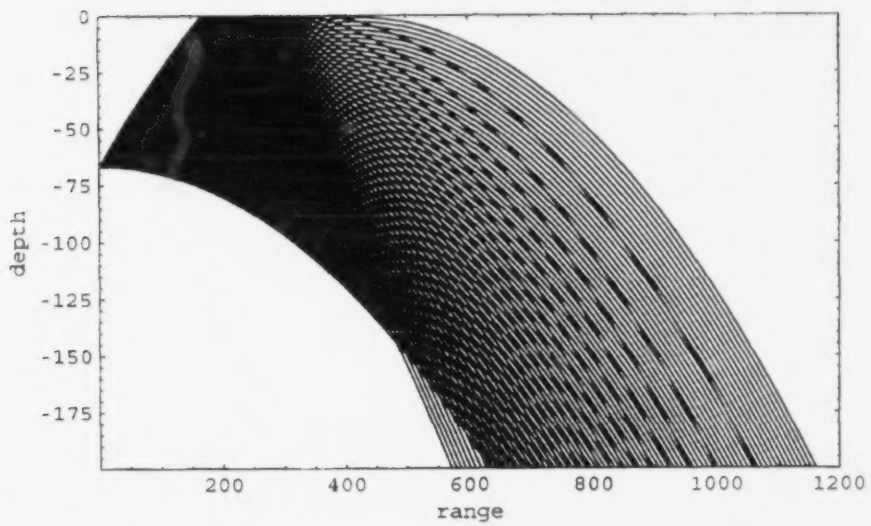

Figure 3.2. The ray trace for the shallow source case for the Gordon and Pedersen profile. The depth and range are in yards.

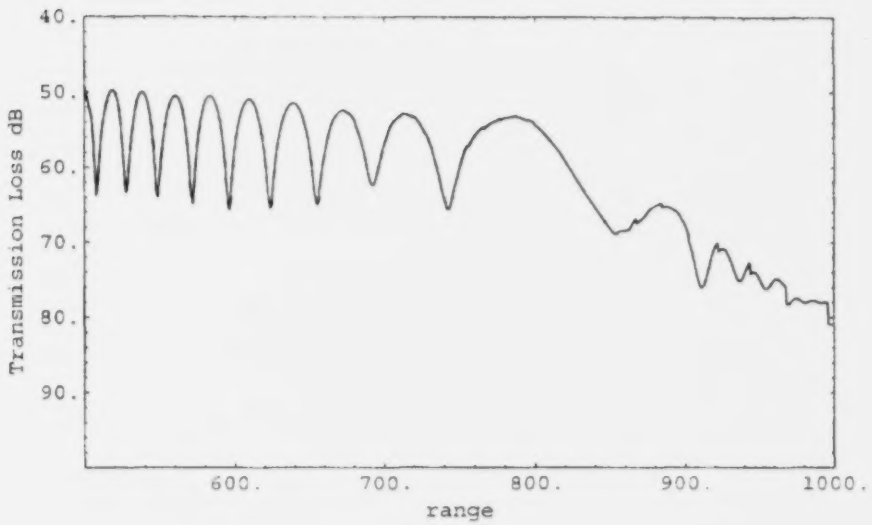

Figure 3.3: The coherent transmission loss for the shallow source case for the Gordon and Pedersen profile, calculated using the Gaussian beam method (Eq. (2.34)). The range is in yards. The parameter values are summarized in Table 3.1. Compare this figure with Fig. 3 (c) of Porter and Bucker[5].

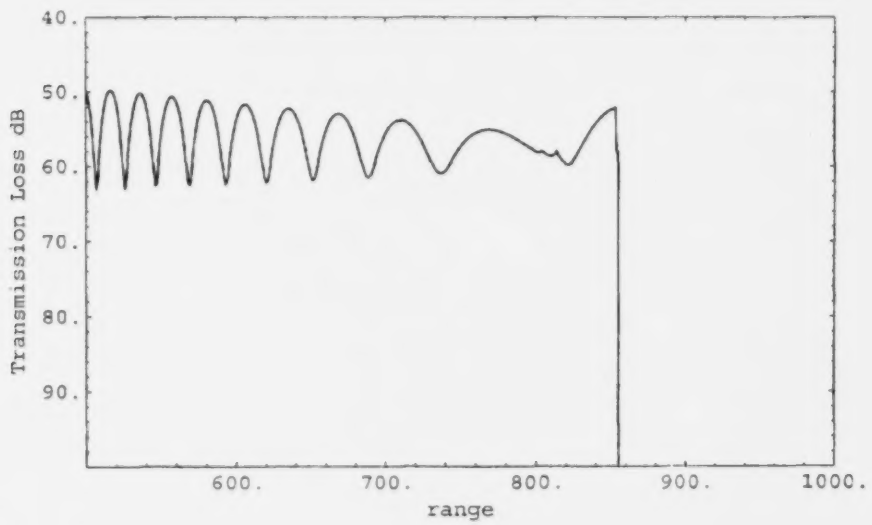

Figure 3.4: The coherent transmission loss for the shallow source case for the Gordon and Pedersen profile, calculated using the classic ray theory method (Eq. (1.14)). The range is in yards. The parameter values are summarized in Table 3.1. Compare this figure with Fig. 3 (a) of Porter and Bucker[5].

P516691 PDF [Page: 33 of 54]

The deep source input parameters are given in Table 3.2. The ray trace for the deep source case is shown

The deep source case:
source depth = 1000 yards
source range =0 yards
receiver depth = 800 yards
receiver range ($3100.0 \leq r \leq 3170.0$) yards
number of beams = 401, $(\theta_i, \theta_f) = (-60.0^o, -20^o)$
frequency = 2000.0 Hz
400 transmission loss points
MaxStepSize→10 yards

Table 3.2: The parameters for the deep source case for the Gordon and Pedersen profile

in Fig. 3.5. The coherent transmission loss calculated using the Gaussian beam method is shown in Fig. 3.6. The classic ray theory result for this case requires the location of caustics, which the contractor has not attempted to incorporate into his software. The classic ray theory result for the deep source case is given in Fig. 5 (a) of Porter and Bucker[5] and Fig. 13 of Gordon and Pedersen[17].

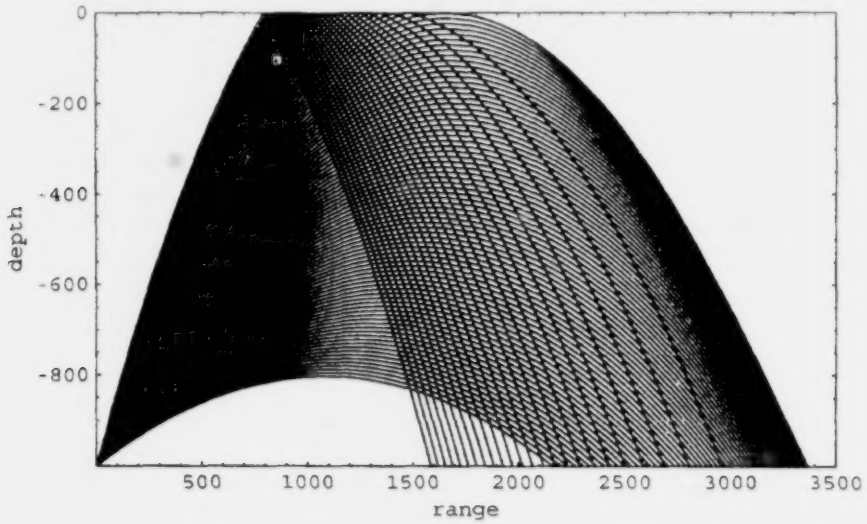

Figure 3.5: The ray trace for the deep source case for the Gordon and Pedersen profile. The depth and range are in yards.

3.2 The Munk Profile

The Munk profile[27] is given by

$$\begin{aligned} c(z) &= 1500\{1.0 + 0.00737[x - 1 + \exp(-x)\},\ z \leq 5000 \text{ m} \\ c(z) &= c(5000), \text{for } z > 5000 \text{ m}. \end{aligned} \tag{3.2}$$

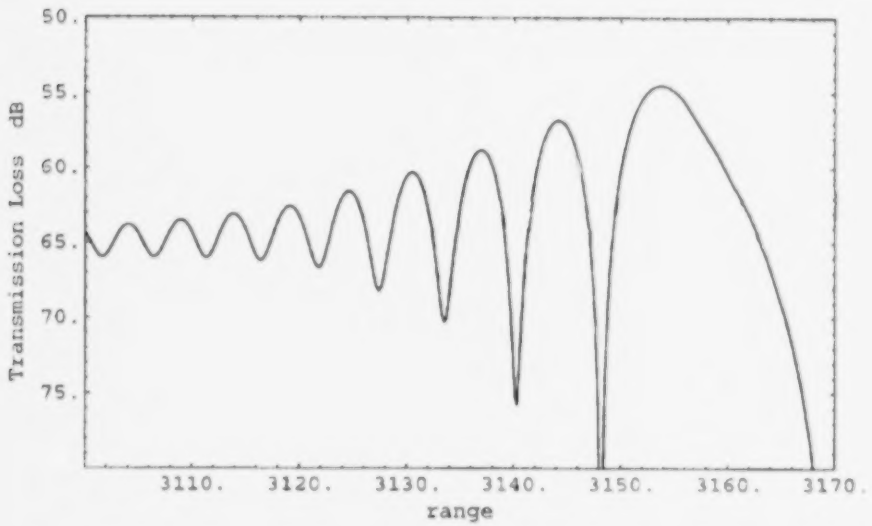

Figure 3.6 The coherent transmission loss for the deep source case for the Gordon and Pedersen profile, calculated using the Gaussian beam method (Eq. (2.34)). The range is in yards. The parameter values are summarized in Table 3.2. Compare this figure with Fig. 5 (c) of Porter and Bucker[5].

where $x = 2(z - 1300)/13000$. A plot of the profile is shown in Fig. 3.7. The Munk case input parameters are given in Table 3.3. The ray trace for the shallow source case is shown in Fig. 3.8. The coherent transmission

The Munk case:
source depth = 1000.0 m
source range =0 yards
receiver depth = 800 m
receiver range $(0.25 \leq r \leq 1000.000)$ m
number of beams = 88, $(\theta_i, \theta_f) = (-14.66°, 14.66°)$
frequency = 50.0 Hz
400 transmission loss points
MaxStepSize→200 m

Table 3.3: The input parameters for the Munk profile case.

loss calculated using the Porter and Bucker method (Eq. (2.34)) is shown in Fig. 3.9, the classic ray theory result is shown in Fig. (3.10).

3.3 Comments on the Gordon and Pedersen and Munk cases

The truly astounding success of the Gaussian beam method is revealed by comparing Fig. 5 (b) of Porter and Bucker with Fig. 3.6. The Gaussian beam method nails the correct benchmark result dead on the money, while a rather difficult application of classic ray theory (including the $-\pi/2$ phase shift for those rays which touch a caustic between source and receiver) is well off the correct result. The ray theory result for the deep

P516691.PDF [Page: 35 of 54]

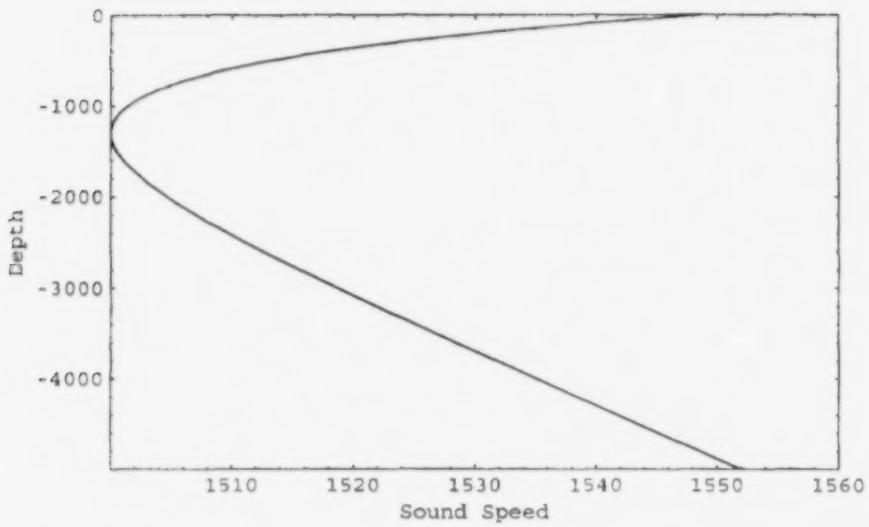

Figure 3.7: The sound speed profile for the Gordon and Pedersen profile. The depth is in meters and the sound speed is meters per second.

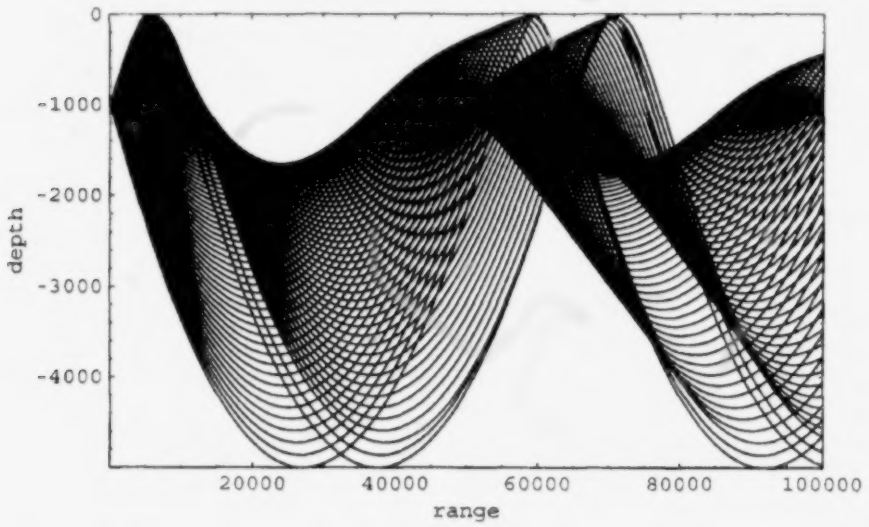

Figure 3.8: The ray trace for the Munk profile. The range and depth are in meters.

P516691.PDF [Page: 36 of 54]

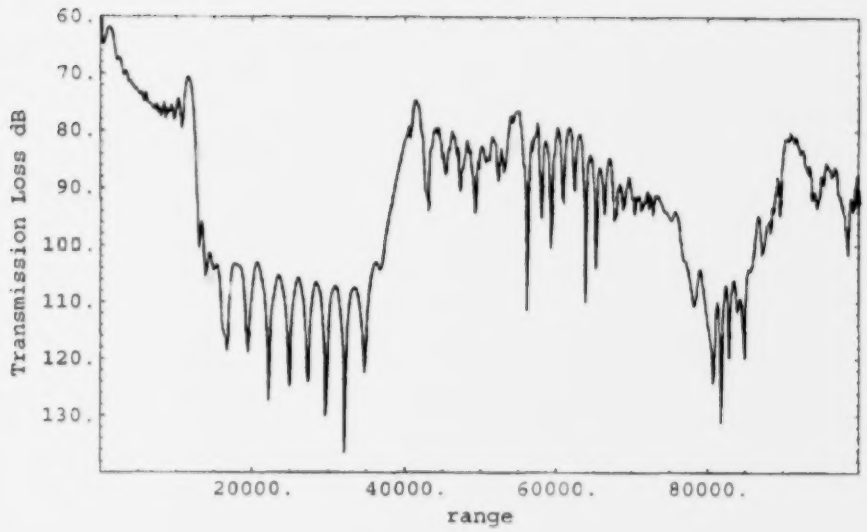

Figure 3.9. The coherent transmission loss for the Munk profile, calculated using the Gaussian beam method. The range is in meters and the input parameters are summarized in Table 3.3. Compare this figure with Fig 8 (c) of Porter and Bucker[5]

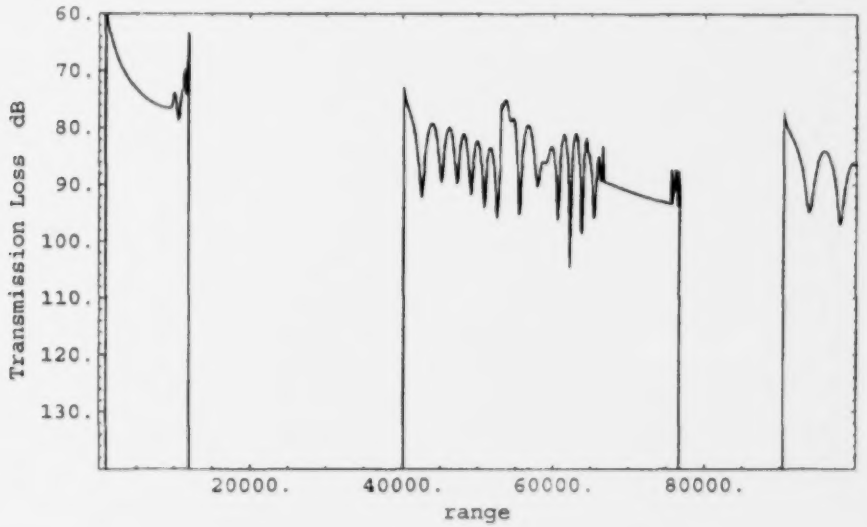

Figure 3.10 The coherent transmission loss for the Munk profile, calculated using the classic ray theory method. The range is in meters and the input parameters are summarized in Table 3 3. Compare this figure with Fig. 8 (a) of Porter and Bucker[5].

P516691.PDF [Page: 37 of 54]

source case requires the location of caustics, which the contractor has not attempted to incorporate in his software. The ray theory result for the deep source result can be found in Fig. 13 of Gordon and Pedersen or Fig. 5.(a) of Porter and Bucker. Hence the classic ray theory result is incorrect even away from the shadow zone. This single case clearly demonstrates the superiority of the Gaussian beam method.

By comparing Fig. (3.3) with the benchmark result Fig. 3 (b) of Porter and Bucker one sees that the Gaussian beam method does not get the transmission loss quite correct deep in the shadow zone, however it is correct as one makes the transition into the shadow zone. (The difference between Porter and Bucker's Fig. 3(c) and Fig. (3.3), which occurs in the shadow zone, is probably due to Porter and Bucker's "windowing" trick, an additional approximation, which the contractor does not carry out.) The Munk case also gives an impressive agreement with the benchmark result given in Fig. 8 (b) of Porter and Bucker. One may also note that the classic ray theory result Fig. 3.10, agrees closely with the Gaussian beam method result Fig. 3.9, away from the shadow zones.

There are certainly some small nagging problems with the Gaussian beam method, such as the correct form of Eq. (2.23) for the range-dependent case, but these do not seem insurmountable.

3.4 The shallow water case: Scenarios 1-5

The five different scenarios to be considered in the course of these ray-theoretic investigations are shown in Fig. (3.11). Scenario 1 has constant sound speed $c = 1500$ m/s and is fairly straight-forward to treat. Scenario 2 has a range independent sound speed Profile A, given by the data points in Table 3.4, and flat ocean surface and ocean bottoms. Again this case can be treated by standard ray theory. Scenario 3 has flat ocean surface and a flat ocean bottom but with a range-dependent sound speed profile, given by a linear interpolation of Profile A into Profile B. Scenario 4 has a flat ocean surface and a variable ocean bottom but with a range-independent sound speed profile, given by Profile A. Scenario 5 has flat ocean surface and a variable ocean bottom but with a range-dependent sound speed profile, given by a linear interpolation of Profile A into Profile B.

Depth (m)	Profile A Sound Speed (m/s)	Profile B Sound Speed (m/s)
0	1511	1498
10	1508	1495
20	1499	1497
30	1490	1490
50	1480	1480
75	1481	1481
100	1488	1488
125	1493	1493
150	1496	1496
200	1497	1497

Table 3.4: The sound speed data for Profiles A and B.

There is the immediate question of how to model the sound speed profiles, whose data points are given in Table 3.4. By inspection of the differential equations of both classic ray theory and the Gaussian beam method one can see that the rhs of these equations depend on up to second derivatives of the sound speed. Strictly speaking, for a well defined mathematical problem one must model the sound speed to have at least

P516691.PDF [Page: 38 of 54]

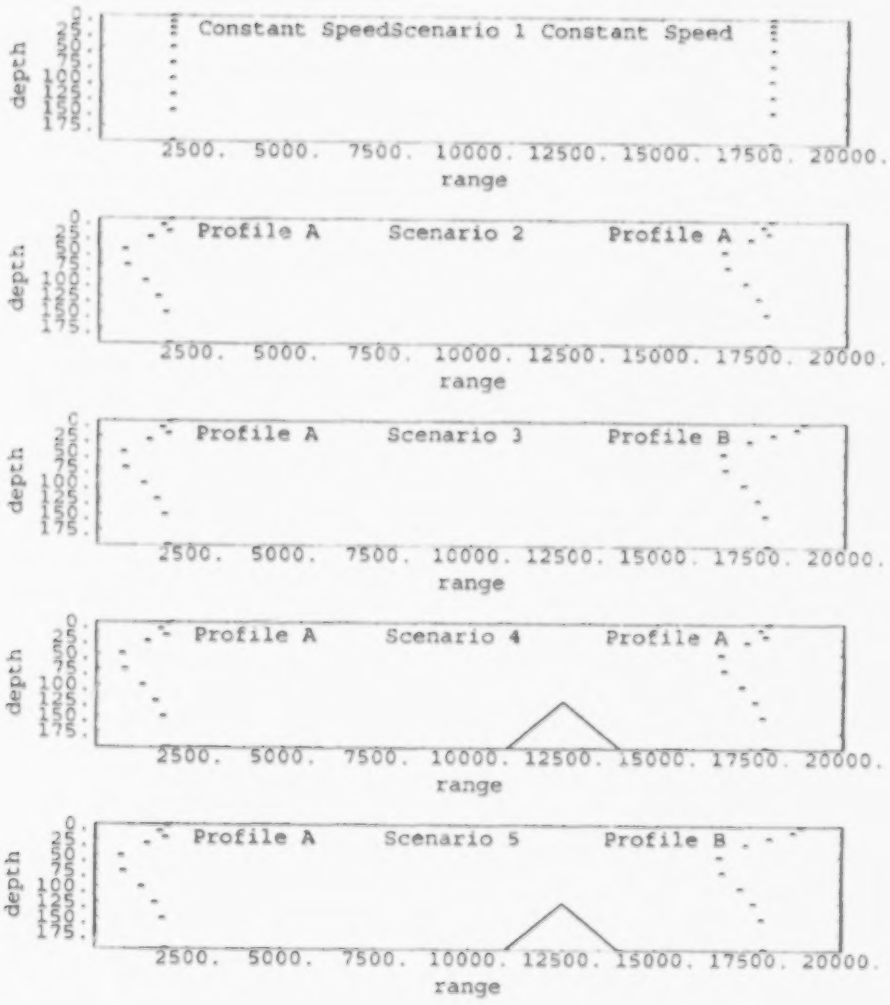
Constant SpeedScenario 1 Constant Speed
Profile A Scenario 2 Profile A
Profile A Scenario 3 Profile B
Profile A Scenario 4 Profile A
Profile A Scenario 5 Profile B
depth
range
2500. 5000. 7500. 10000. 12500. 15000. 17500. 20000.

Figure 3.11: Shallow water scenarios for ray theoretic analysis

P516691.PDF [Page: 39 of 54]

continuous first and second derivatives. For example, consider what happens when one linearly interpolates between sound speed data points and then puts a source at that data point depth. The derivative $c_z(r,z)$ will have a discontinuity, on the other hand $c_z(r,z)$ occurs as an input function in the ray equations. Furthermore, when the initial angle of the ray is horizontal one has (in the numerical solution of the differential equations)

$$\delta z \approx \delta s \frac{dz}{ds} = \sin(\theta)\delta s = 0.$$

So not only do you not know what the value of c_z is at that initial depth, but you are stuck at that depth, for rays that initially moving horizontally. The problems associated with discontinuities in the sound speed have been pointed out by Pedersen[28]. Ideally one should fit the data to smoothly varying functions rather than interpolate. That said, one can easily construct a piecewise interpolation scheme in Mathematica (in which one specifies the first and second derivatives explicitly) which guarantees that the first and second derivatives wrt r and z are continuous. However the mathematical price that one pays for this scheme, is that the sound speed profile ends up with an incredible amount of small scale variation wrt to depth. The numerical solution of the differential equations slows down (by a factor of fifty or so), so this is not a pleasant option. The correct procedure to fit the data rather than interpolate the data. The difficulty is choosing a set of smoothly varying functions to use in the (least squares fit).

By analogy with the Munk case, the contractor has chosen a sum of exponential functions in the form

$$c(z) = a_1 + a_2 z + a_3 z^2 + a_4 * z^3 + a_5 e^{-a_6 z} + a_7 e^{-a_8 z} + a_9 e^{-a_{10} z}. \tag{3.3}$$

A least squares fit of the Profile A and B sound speed data to these functional forms is shown in Figs. (3.12). Since only two data points are given in range, one assumes a linear variation with range. Details are given in the contractor software.

The investigations of ray theoretic methods in this contract may be divided roughly into two parts. The first part is the determination of the classic ray paths, grazing angles and travel times for a range-independent profile, variable bathymetry environment. The second part, more recondite than the first, is the determination of the coherent transmission loss, either with classic ray methods (Eq (1.14)) or Gaussian beam theory (Eq. (2.34)). The first part has been solved completely by the contractor, the software provided can track multiple bounces from rough bottom, range-dependent sound speed environments. A few examples of ray traces are shown in Figs. (3.13)-(3.16). One may also extract the numerical values of such parameters as grazing angle, travel times etc. in tabular form for subsequent use.

In hindsight, the most difficult transition to make is go from Scenario 3 (the flat ocean bottom) to Scenario 4 (variable bathymetry), and find a robust numerical technique to keep track of the multi-path arrivals. Scenario 4 requires some degree of sophistication to properly keep track of the bottom and surface bounces and the multipath arrivals, however there are no conceptual difficulties. Scenario 5 has a range-dependent profile and variable bathymetry. Again, once one has in place the machinery to properly handle the surface and bottom bounces and all the multipath arrivals, the extension to a range-dependent environment is straightforward. Very briefly, to track the multipath arrivals including reflections, the contractor has used the undocumented option StoppingTest in the Mathematica function NDSolve[ ]. One is then able to extract the last four arclength values found in the numerical solution of the ray equations during a particular leg of a ray path. The last value of arclength invokes the Stopping condition at a boundary, and corresponds to penetration through the boundary. Hence this value cannot be used as the starting point of a new leg of the ray path. Instead one manipulates the last four values of arclength found by NDSolve[ ] to reconstruct the

PS16691 PDF [Page: 40 of 54]

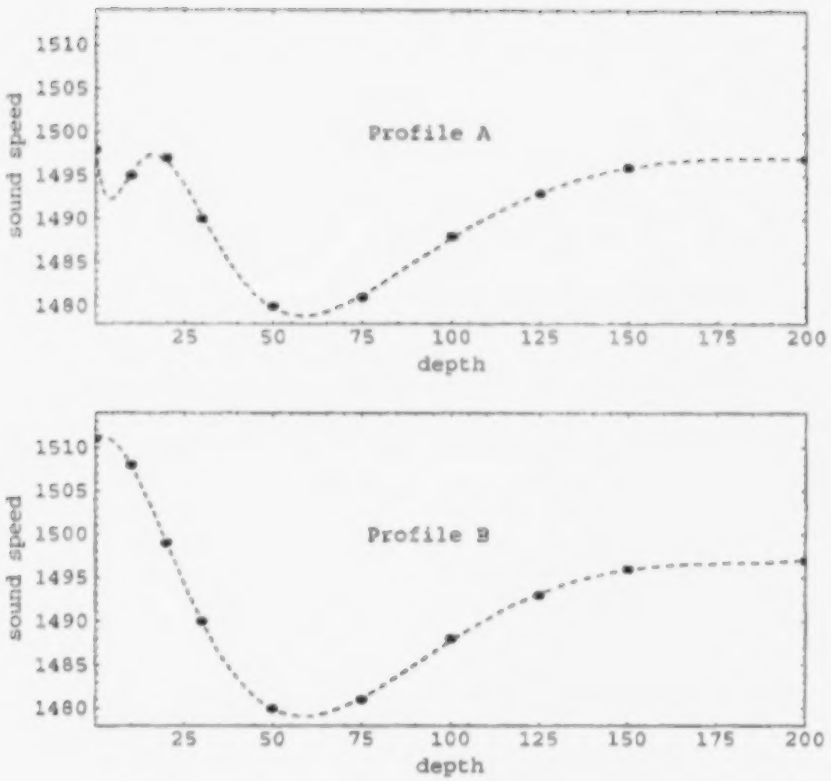

Figure 3.12: A least squares fit of exponentials (see Eq. (3 3)) to the data in Table 3 4 The depth is in meters and the sound speed is in meters per second.

P516691.PDF [Page: 41 of 54]

cubic interpolating polynomial used in the solution of the differential equations by Mathematica. One then solves for the exact intersection of this (Lagrange) cubic interpolating polynomial with the boundaries to find the value of arclength to be used as the new starting value for the next leg of the ray path. In addition one construct a similar scheme for all the other parameters $r(\theta, s)$, $z(\theta, s)$ and so on. This gives the new starting values for the next leg of a ray path after a reflection from an arbitrary rough surface. By adding various counter variables and Throw[] functions, one is able to terminate a ray after a selected number of surface and bottom bounces. Programming details are given in the software. A number of test ray traces are shown in Figs. 3.13-3.16. One interesting feature of the ray trace is appearance of an "image" of the triangular-shaped bottom irregularity in Scenario 5. in the subsequent ray trace pattern. For example, this appears as triangular-shaped "quiet zone" at a range of 15,000 m in Fig. 3.16. This feature appears as a notch in the coherent transmission loss in Fig. 3.18. at range $\approx$ 15,000 m.

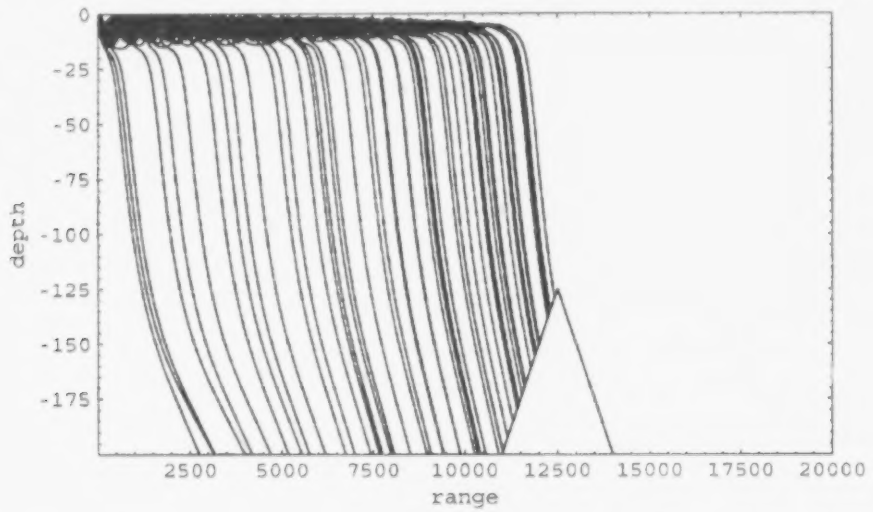

Figure 3.13. The ray trace for Scenario 5, for a source located in the upper duct at depth $z = 5$ m. There are 51 rays evenly spaced between $-5^o \leq \theta \leq 5^o$.The rays are terminated after 1 surface or 1 bottom bounce.

The second part of this contract, the calculation of coherent transmission loss, has certain limitations. Firstly in classical ray theory, since Ugincius has not generalized Eqs. (1.23)-(1.25) to arbitrary rough surfaces, one is limited to either a flat ocean bottom or else to terminate all rays after a single bottom bounce from the rough surface, or calculate the derivatives $dr/d\theta$ etc. using finite differences as in Eq. (1.26). Secondly, as pointed out by Porter and Bucker and verified by the contractor, Eq. (60) of Cerveny[2] is incorrect when reduced to the special case of a flat surface. Porter and Bucker found an empirical solution to this problem for the range-independent, flat surface case. However this calls into question Cerveny's more general results for arbitrary bathymetry, range-dependent environments as well. In effect, this limits the Cerveny method to a single bottom bounce from a rough surface. With this in mind the contractor has used the Gaussian beam method and the classic ray theory to calculate the coherent transmission loss for Scenario 5, where all rays are terminated after one surface or one bottom bounce. The Scenario 5 input parameters are given in

P516691.PDF [Page: 42 of 54]

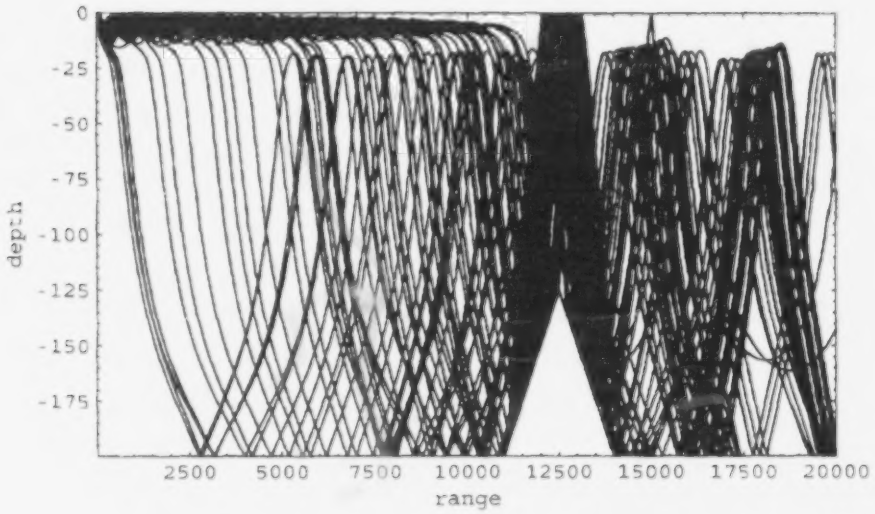

Figure 3.14: The ray trace for Scenario 5, for a source located in the upper duct at depth $z = 5$ m. There are 51 rays evenly spaced between $-5^o \leq \theta \leq 5^o$. The rays are terminated after 100 surface or 4 bottom bounces.

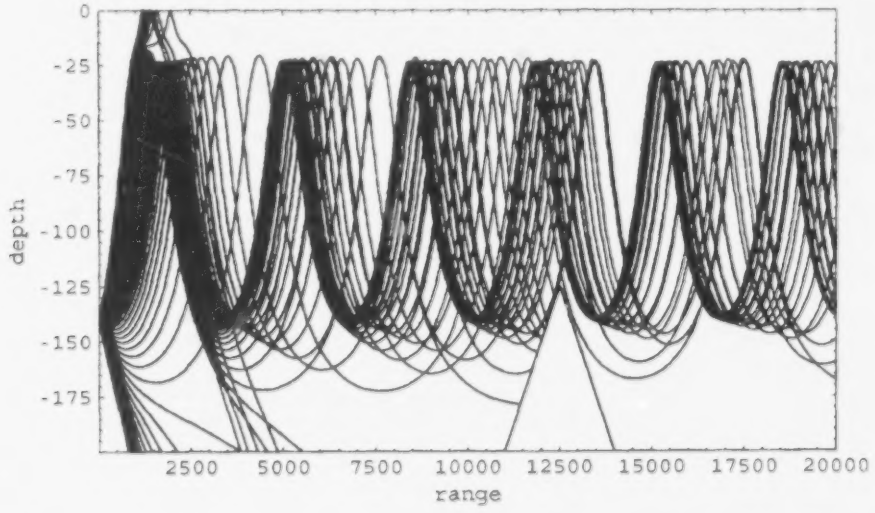

Figure 3.15: The ray trace for Scenario 5, for a source located in the lower duct at depth $z = 140$ m. There are 51 rays evenly spaced between $-5^o \leq \theta \leq 5^o$. The rays are terminated after 1 surface or 1 bottom bounce.

P516691.PDF [Page: 43 of 54]

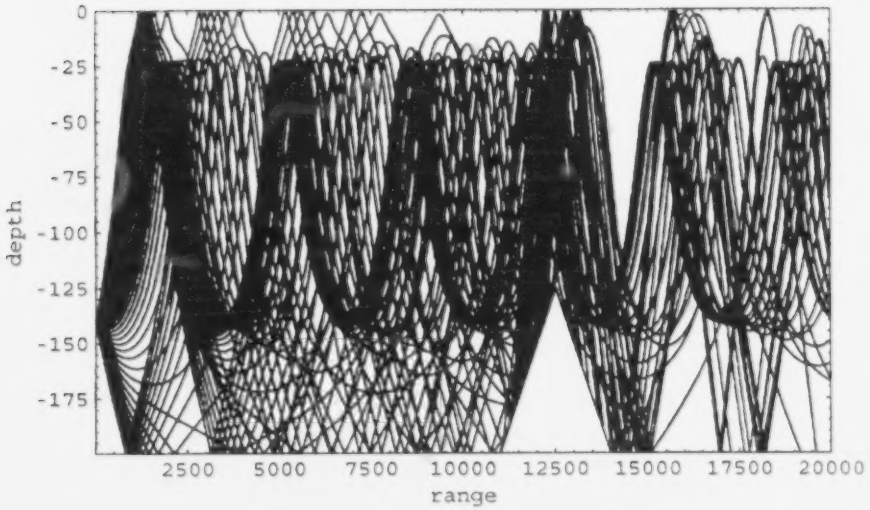

Figure 3.16. The ray trace for Scenario 5, for a source located in the lower duct at depth $z = 140$ m. There are 51 rays evenly spaced between $-5^\circ \leq \theta \leq 5^\circ$. The rays are terminated after 100 surface or 4 bottom bounces.

Table 3.5. The results are shown in Figs 3.17 and 3.18.

Scenario 5:
source depth = 140.0 m
source range =0 yards
receiver depth = 75 m
receiver range $(0 \leq r \leq 20{,}000)$ m
number of beams = 501. $(\theta_i, \theta_f) = (-5.0^\circ, 5.0^\circ)$
frequency = 1000.0 Hz
800 transmission loss points
MaxStepSize→ Infinity

Table 3.5: The input parameters for Scenario 5

Comments: the Gaussian ray method and the classic ray method give comparable results over shorter ranges, corresponding to a few turning points of the ray paths. However the classic ray theory gives much higher levels than the Gaussian beam method after about 4 or 5 ray turning points. At this stage the contractor does know where the discrepancy lies. The ray method and the Gaussian beam method certainly give very similar results over a few turning points for the Gordon Pedersen case and the Munk case. Compare for example Figs. 3.3 and 3.4 and Figs 3.9 and 3.10. Away from the shadow zones the predictions of Eq. (1.14) and Eq. (2.34) are very close for these cases. The differences at longer ranges between the predictions of Eq. (1.14) and Eq. (2.34) are not due to variable bathymetry effects or the range-dependent sound speed effects of Scenario 5. These same difference at longer ranges persist even in the case of Scenario 2 (not shown). What is required to sort out these differences is a comparison of ray theory and Gaussian beam

P516691.PDF [Page: 44 of 54]

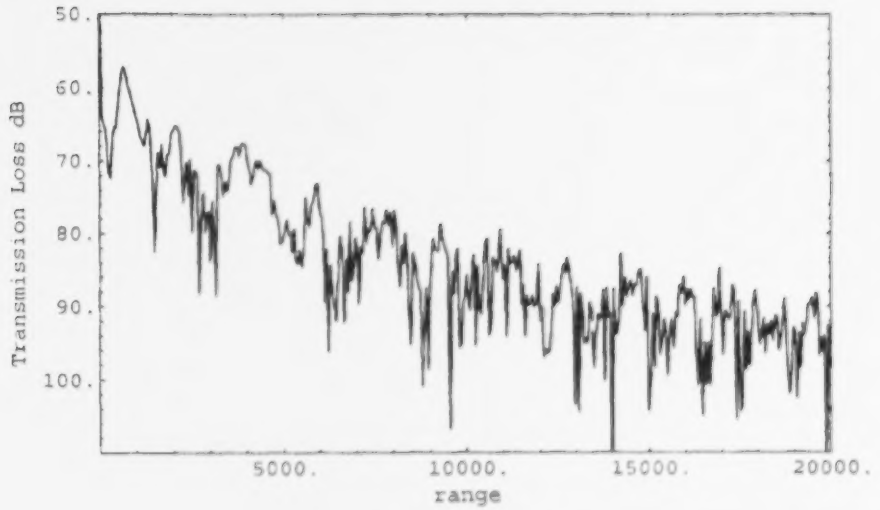

Figure 3.17: The coherent transmission loss for the deep source case for Scenario 5, calculated using the Gaussian beam method. There are 501 rays evenly distributed over initial angles $-5^o \leq \theta \leq 5^o$. The rays are terminated after 1 surface or 1 bottom bounce. The input parameters are given in Table 3.5.

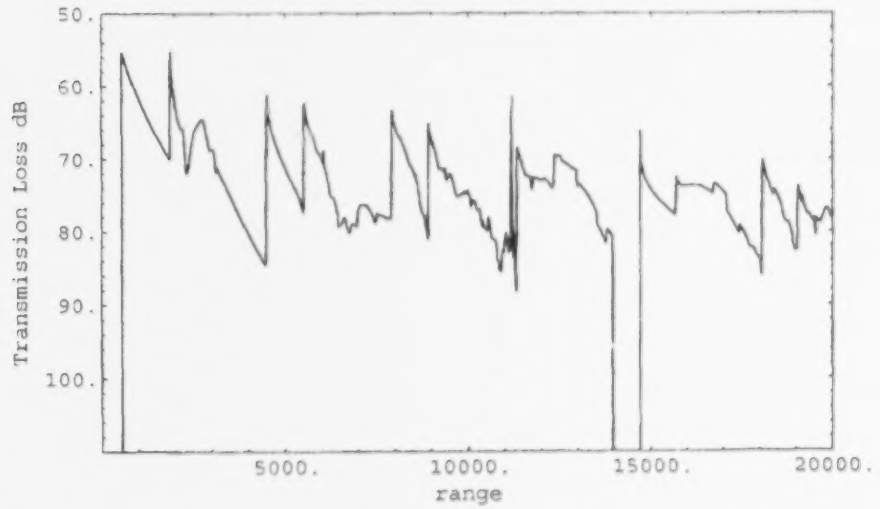

Figure 3.18: The coherent transmission loss for the deep source case for Scenario 5, calculated using the classic ray theory method. There are 501 rays evenly distributed over initial angles $-5^o \leq \theta \leq 5^o$. The rays are terminated after 1 surface or 1 bottom bounce. The input parameters are given in Table 3.5

theory at longer ranges, including many ray turning points. For example one could re-examine the Munk case at much longer ranges. Given the limited time resources at the contractors disposal, the best that can be said is that the classic ray theory and the Gaussian beam method gives comparable results over a few ray turning points. The case of longer ranges needs further study and comparison with benchmark results.

Chapter 4

CONCLUSIONS

Comments on the application of classic ray theory to range-dependent sound speed profile and variable bathymetry (cylindrical symmetry) environments:

(1) The calculation of the ray paths, arrival angles and travel times for the Scenario 5 environment is completely tractable with classic ray theory and working software has been provided by the contractor.

(2) The machinery used to treat the variable bathymetry problem within the framework of classic ray theory, may be transferred in toto to the Gaussian beam method.

(3) The most difficult feature of classic ray theory calculations of transmission loss is the inversion problem; this problem is closely linked to the problem of interpolating between rays with neighboring values of initial grazing angles. There is room for a considerable improvement in this interpolation process by constructing a scheme which interpolates along curves of constant local grazing angle $\phi(\theta, s)$.

(4) There is a huge numerical advantage in solving the ray equations with a sound speed profile which has been fitted rather than interpolated. Requiring continuity of first and second derivatives of the sound speed (which is required in calculating transmission losses) creates an interpolating function with considerable small scale variation. This in turn slows down the numerical solution of the differential ray equations. When modeling sound speed data, fit don't interpolate.

Comments on the application of the Gaussian beam method to range-dependent sound speed profile and variable bathymetry (cylindrical symmetry) environments:

(1) The Gaussian beam method gives impressive agreement with the deep source case for the Gordon and Pedersen profile, a case that resists treatment by classic ray theory, even when caustics are treated correctly.

(2) There is no inversion problem as in classic ray theory, only the more tractable problem of finding the normal distances from the field point to the beam centers.

(3) The Gaussian beam method does not give completely correct results deep in the shadow zone, but it does give correct values for transmission losses as the range makes the transition just past the shadow zone.

(4) It is a relatively straight forward programming problem to numerically implement the Gaussian beam method.

(5) There is a problem concerning the correct form of the boundary conditions for the p variable in the range-dependent case. Cerveny's boundary condition for the " p" variable, Eq.(60) of [2], is incorrect, and his derivation needs to be re-examined in detail. The scope of the effort required to fix this problem is unknown. A promised paper on this subject by Porter and Bucker was not published. To properly apply the

Gaussian beam method to variable-bathymetry, range-dependent cases, where the interaction of multi-path reflected beams is accounted for, this issue must be resolved.

General comments: Classic ray theory and Gaussian beam calculations of the coherent transmission loss give similar results for the Gordon and Pedersen, Munk profiles and Scenario 5 cases when compared over ranges of a few ray turning points. For ranges involving many ray turning points, the classic ray theory gives much higher levels than Gaussian beam theory for Scenario 5. This suggests a re-examination of benchmark cases over much longer ranges to resolve this discrepancy.

P516691.PDF [Page: 48 of 54]

ACKNOWLEDGEMENTS

The author would like to thank Dave Chapman and Jim Theriault of the Defence Research Establishment Atlantic for their assistance. This work was funded by the Defence Research Establishment Atlantic under contract number W7707-00-8696.

P516691.PDF [Page: 49 of 54]

Bibliography

[1] V. Cerveny, M. M. Popov and I. Psencik, "Computation of wave fields in inhomogeneous media–Gaussian beam approach," Geophys. J. R. astr. Soc. **70**, 109–128 (1982).

[2] V. Cerveny and I. Psencik, "Gaussian beams in elastic 2-D laterally varying layered structures," Geophys. J. R. astr. Soc. **78**, 65–91 (1984).

[3] V. Cerveny and J. E. P. Soares, "Fresnel volume ray tracing," Geophysics **57**, 902–915 (1992).

[4] V. Cerveny, L. Klimes and I. Psencik, "Paraxial ray approximations in the computation of seismic wavefields in inhomogeneous media," Geophys. J. R. astr. Soc. **79**, 89–104 (1984).

[5] M. B. Porter and H. P. Bucker, "Gaussian beam tracing for computing ocean acoustic fields," J. Acoust. Soc. Am. **82**, 1349–1359 (1987).

[6] H. P. Bucker, "A simple 3-D Gaussian beam sound propagation model for shallow water," J. Acoust. Soc. Am. **95**, 2437–2440 (1994).

[7] M. B. Porter and Y-C Liu, "Finite-element ray tracing," Theoretical and Computational Acoustics, **2**, D. Lee and M. H. Shultz (Editors), World Scientific Publishing Company, pp. 947-956, 1994.

[8] H. Weinberg and R. Keenan, "Gaussian ray bundles for modeling high-frequency propagation loss under shallow-water conditions," J. Acoust. Soc. Am. **100**, 1421–1431 (1996).

[9] Lawrence E. Kinsler, Austin R. Frey, Alan B. Coppens, and James V. Saunders, *Fundamentals of Acoustics, Third Edition*, (Wiley and Sons, 1982).

[10] P. Ugincius, "Intensity Equations in Ray Acoustics," J. Acoust. Soc. Am. **45**, 193–205 (1969).

[11] P. Ugincius, "Intensity Equations in Ray Acoustics. II," J. Acoust. Soc. Am. **45**, 206–341 (1969).

[12] P. Ugincius, "Intensity Equations in Ray Acoustics. III. Exact Two-Dimensional Formulation," J. Acoust. Soc. Am. **47**, 339–341 (1970).

[13] E. S. Eby and L. T. Einstein, "General Spreading Loss Expression," J. Acoust. Soc. Am. **37**, 933–944 (1965).

[14] G. Anderson, R. Gocht, and D. Sirota, "Spreading Loss of Sound in an Inhomogeneous Medium," J. Acoust. Soc. Am. **36**, 140–145 (1964).

[15] K. Chen and D. Ludwig, "Calculation of wave amplitudes by ray tracing," J. Acoust. Soc. Am. **54**, 431–436 (1973).

[16] R. F. MacKinnon,J. S. Partridge, and S. H. Toole, "On the Calculation of Ray-Acoustic Intensity," J. Acoust. Soc. Am. **52**, 1471–1480 (1972).

[17] M. A. Pedersen and D. F. Gordon, "Normal-Mode and Ray Theory Applied to Underwater Acoustic Conditions of Extreme Downward Refraction," J. Acoust. Soc. Am. **51**, 323–368 (1972).

[18] S. Wolfram, *The Mathematica Book, 3rd ed.*, (Wolfram Media/Cambridge University Press, 1996).

[19] D. J. Thompson, "Wide-angle parabolic equation solutions to two range-dependent benchmark problems," J. Acoust. Soc. Am. **87**, 1514-1520 (1990).

[20] D. J. Thompson, G. H. Brooke, and J. A. DeSanto, "Numerical implementation of a modal solution to a range-dependent benchmark problem," J. Acoust. Soc. Am. **87**, 1521-1526 (1990).

[21] M. J. Buckingham and Alexandra Tolstoy, "An analytical solution for benchmark problem 1: The "ideal" wedge," J. Acoust. Soc. Am. **87**, 1511-1513 (1990).

[22] M. D. Collins, "Benchmark calculations for higher-order parabolic equations," J. Acoust. Soc. Am. **87**, 1535-1538 (1990).

[23] E. K. Westwood, "Ray model solutions to the benchmark wedge problems," J. Acoust. Soc. Am. **87**, 1539-1545 (1990).

[24] F. B. Jensen and C. M. Ferla, "Numerical solutions of range-dependent benchmark problems in ocean acoustics," J. Acoust. Soc. Am. **87**, 1499-1510 (1990).

[25] R. A. Stephen, "Solutions to range-dependent benchmark problems by the finite-difference method," J. Acoust. Soc. Am. **87**, 1527-1534 (1990).

[26] P. A. Baxely, H. Bucker and M. B. Porter, "Comparison of beam tracing algorithms," *Proceedings of the Fifth European Conference on Underwater Acoustics, ECUA 2000. Editor: M. E. Zakharia, c-editors: P. Chevet, P. Dubail, Lyon, France, 2000*, p.27–33.

[27] W. H. Munk, "Sound channel in an exponentially stratified ocean, with application to SOFAR," J. Acoust. Soc. Am. **55**, 220–226 (1974).

[28] M. A. Pedersen, "Acoustic Intensity Anomalies Introduced by Constant Velocity Gradients," J. Acoust. Soc. Am. **33**, 465–474 (1961).

[29] H. Weinberg and R. Keenan, "A Continuous-Gradient Curve-Fitting Technique for Acoustic Ray Analysis," J. Acoust. Soc. Am. **50**, 975–984 (1971).

[30] H. Weinberg, "Application of ray theory to acoustic propagation horizontally stratified oceans," J. Acoust. Soc. Am. **58**, 97–109 (1975).

[31] H. Weinberg, "Effective range derivative for acoustic propagation loss in a horizontally stratified ocean," J. Acoust. Soc. Am. **70**, 1736–1742 (1981).

P516691.PDF [Page: 51 of 54]

[32] P.E Etter, "Challenges in Environmental Acoustics," Proc. Oceans 200, Vol. 2, 877-886 (2000).

[33] R. E Keenan, "An Introduction to GRAB Eigenrays and Cass Reverberation and Signal Excess," Proc. Oceans 2000, Vol 2, 1065-1070 (2000).

[34] H. Weinberg, "CASS Roots," Proc. Oceans 2000, Vol 2, 1071-1076 (2000).

[35] L. B. Felsen, "Geometrical theory of diffraction, evanescent waves, complex rays and Gaussian beams," Geophys. J. R. astr. Soc. **79**, 77-88 (1984).

UNCLASSIFIED
SECURITY CLASSIFICATION OF FORM
(highest classification of Title, Abstract, Keywords)

DOCUMENT CONTROL DATA

(Security classification of title, body of abstract and indexing annotation must be entered when the overall document is classified)

1 ORIGINATOR (the name and address of the organization preparing the document. Organizations for whom the document was prepared, e.g. Establishment sponsoring a contractor's report, or tasking agency, are entered in section 8.)

Anthony Purcell, Anthony Purcell Consultants
PO Box 1388, Lunenburg, NS B0J 2C0

2 SECURITY CLASSIFICATION (overall security classification of the document including special warning terms if applicable)

Unclassified

3 TITLE (the complete document title as indicated on the title page. Its classification should be indicated by the appropriate abbreviation (S,C,R or U) in parentheses after the title)

Investigation of Range-Dependent Underwater Acoustic Ray Models

4 AUTHORS (Last name, first name, middle initial. If military, show rank, e.g. Doe, Maj. John E.)

Purcell, Anthony

5 DATE OF PUBLICATION (month and year of publication of document)

September 2001

6a NO. OF PAGES (total containing information. Include Annexes, Appendices, etc.)

45

6b NO. OF REFS (total cited in document)

35

7 DESCRIPTIVE NOTES (the category of the document, e.g. technical report, technical note or memorandum. If appropriate, enter the type of report, e.g. interim, progress, summary, annual or final. Give the inclusive dates when a specific reporting period is covered.)

Contractor Report

8 SPONSORING ACTIVITY (the name of the department project office or laboratory sponsoring the research and development. Include address.)

Defence Research Establishment Atlantic
P.O. Box 1012
Dartmouth, NS B2Y 3Z7

9a PROJECT OR GRANT NO. (if appropriate, the applicable research and development project or grant number under which the document was written. Please specify whether project or grant.)

11cc

9b CONTRACT NO. (if appropriate, the applicable number under which the document was written.)

W7707-00-8696

10a ORIGINATOR'S DOCUMENT NUMBER (the official document number by which the document is identified by the originating activity. This number must be unique to this document.)

DREA CR 2001-136

10b OTHER DOCUMENT NOs. (Any other numbers which may be assigned this document either by the originator or by the sponsor.)

11 DOCUMENT AVAILABILITY (any limitations on further dissemination of the document, other than those imposed by security classification)

(X) Unlimited distribution
( ) Defence departments and defence contractors; further distribution only as approved
( ) Defence departments and Canadian defence contractors; further distribution only as approved
( ) Government departments and agencies; further distribution only as approved
( ) Defence departments; further distribution only as approved
( ) Other (please specify): informal publication in draft format only for limited distribution

12 DOCUMENT ANNOUNCEMENT (any limitation to the bibliographic announcement of this document. This will normally correspond to the Document Availability (11). However, where further distribution (beyond the audience specified in (11) is possible, a wider announcement audience may be selected.)

No

UNCLASSIFIED
SECURITY CLASSIFICATION OF FORM

UNCLASSIFIED
SECURITY CLASSIFICATION OF FORM
(highest classification of Title, Abstract, Keywords)

P516691.PDF [Page: 53 of 54]

13. ABSTRACT (a brief and factual summary of the document. It may also appear elsewhere in the body of the document itself. It is highly desirable that the abstract of classified documents be unclassified. Each paragraph of the abstract shall begin with an indication of the security classification of the information in the paragraph (unless the document itself is unclassified) represented as (S), (C), (R), or (U). It is not necessary to include here abstracts in both official languages unless the text is bilingual)

This report is an annotated bibliography of ray theory approaches to the analysis of high frequency, shallow water propagation. Specifically, it is concerned with the calculation of the ray paths, travel times, arrival angles and coherent transmission losses for range-dependent velocity profile, variable bathymetry, and shallow water environments. The two approaches considered are the classic ray theory and the Gaussian beam method. The software developed in this report to evaluate the feasibility of applying these models to range-dependent environments is based on the numerical solution of the differential ray equations rather than analytic solutions of the ray paths for special cases. The ocean surface is assumed to be a flat pressure-release surface; the ocean bottom is a rigid, arbitrary bathymetry surface. The number of allowed surface or bottom bounces is adjustable and arbitrary. All parameters have cylindrical symmetry so there is propagation only in the same plane. The specific cases considered are the Gordon and Pedersen profile, the Munk profile, and a range-dependent, variable bathymetry, shallow water environment referred to as Scenario 5.

14. KEYWORDS, DESCRIPTORS or IDENTIFIERS (technically meaningful terms or short phrases that characterize a document and could be helpful in cataloguing the document. They should be selected so that no security classification is required. Identifiers, such as equipment model designation, trade name, military project code name, geographic location may also be included. If possible keywords should be selected from a published thesaurus, e.g. Thesaurus of Engineering and Scientific Terms (TEST) and that thesaurus-identified. If it not possible to select indexing terms which are Unclassified, the classification of each should be indicated as with the title)

ray theory
travel time
transmission loss
range-dependent modeling
variable bathymetry
Gaussian beam method
underwater acoustics
Mathematica
Munk profile
Gordon and Pedersen profile

Defence R&D Canada
is the national authority for providing
Science and Technology (S&T) leadership
in the advancement and maintenance
of Canada's defence capabilities.

R et D pour la défense Canada
est responsable, au niveau national, pour
les sciences et la technologie (S et T)
au service de l'avancement et du maintien des
capacités de défense du Canada.

516691

CA020027

DEFENCE R&D DÉFENSE

www.drdc-rddc.dnd.ca